

Performance Analysis of Wireless and Dispersion Compensated Optical Communications System

A DISSERTATION

SUBMITTED IN PARTIAL FULFILMENT OF THE REQUIREMENTS
FOR THE AWARD OF THE DEGREE
OF

MASTER OF TECHNOLOGY
IN
MICROWAVE AND OPTICAL COMMUNICATIONS

Submitted by:

DIVYA SISODIYA

2K20/MOC/03

Under the supervision of

DR. DEEPIKA SIPAL



ELECTRONICS AND COMMUNICATIONS ENGINEERING

DELHI TECHNOLOGICAL UNIVERSITY

Formerly Delhi college of Engineering

Bawana Road, Delhi-110042

May, 2022

**DEPARTMENT
OF
ELECTRONICS AND COMMUNICATIONS ENGINEERING
Delhi Technological University
(Formerly Delhi college of Engineering)
Bawana Road, Delhi-110042**

CANDIDATE'S DECLARATION

I, Divya Sisodiya (2K20/MOC/03) students of M. Tech (Microwave and Optical Communication Engineering), hereby declare that the Report titled “**performance analysis of wireless and dispersion compensated optical communications system**” which is submitted by me to the Department of Electronics and Communication Engineering, Delhi Technological University, Delhi in partial fulfilment of the prerequisite for the granting of degree of Master of Technology, is unique and not plagiarised from any source without appropriate attribution. This work has never before served as the foundation for the award of a degree, diploma, associateship, fellowship, or other equivalent title or honour.

Place: Delhi
Date: 31/05/2022

(DIVYA SISODIYA)

**DEPARTMENT
OF
ELECTRONICS AND COMMUNICATIONS ENGINEERING
Delhi Technological University
(Formerly Delhi college of Engineering)
Bawana Road, Delhi-110042**

CERTIFICATE

I hereby certify that the report titled “**performance analysis of wireless and dispersion compensated optical communications system**” which is submitted by **Divya Sisodiya** (2K20/MOC/03) in Department of Electronics and Communication Engineering, **Delhi Technological University**, Delhi in partial fulfilment of the prerequisite for the granting of degree of Master of Technology, is a documentation of the project work completed by student under my guidance. To the best of my knowledge, this work has not been submitted in part or in full for any Degree or Diploma at this University or elsewhere.

Place: Delhi
Date: 25/11/21

(Dr Deepika Sipal)
Supervisor

ACKNOWLEDGEMENT

The success and ultimate outcome of this project need a great deal of direction and assistance from many individuals, and I am lucky to be able to fulfil all of this while finishing my project work. Everything I accomplish is due to such instruction and assistance. I shall not forget to thank everyone.

I am most grateful for my Asst project guide. Professor Deepika Sipal gave me the opportunity to do this job. Dr. Deepika Sipal was highly interested in my research project and supported me through the entire process till it was finished, providing me with all the necessary information, continuous encouragement, sincere criticism, and an understanding attitude.

Place: Delhi
Date: 31/05/2022

(DIVYA SISODIYA)

ABSTRACT

A communication system in which light is used to carry a stream of information is called Optical Communication System. A modern optical communication system consists of optical fiber, optical amplifier, switches, laser and different advanced technologies for setup a communication link. In this dissertation most of the work focuses on the performance analysis of fiber optical communication system and wireless optical communication system.

Over long transmission distances, the use of an erbium-doped fiber amplifier (EDFA) reduces attenuation in the information signal. Non-linearities in the fiber cause dispersion. Some common techniques for reducing dispersion effects in fiber-optic communications are dispersion compensated fiber (DCF) and fiber Bragg gratings (FBG). The research nowadays focuses more on less complex system with higher achievable data rates and optical wireless communications (OWC) is a viable alternative for both inside and outside high-speed wireless access. These laser-based systems provide a low-cost framework link with high data rates (up to 10 Gbit/s) and could be a solution to the high bandwidth constraint.

The first part research work of this dissertation describes different types of DCF techniques using cascaded uniform and chirped FBGs. The proposed models are composed of four consecutive uniform FBGs connected to the transmitter. The transmitter is modulating the amplitude of signal and the use of DCF with cascaded FBG enhances the overall system performance. No matter how much dispersion is reduced but the fibre optical communication has issues of complexity, high cost of implementation and prone to cable damage (interference) while implementing them physically. So, the next part of the project focuses on wireless optical communications like OWC channel which can reduce the issues of fibre optic communications. OWC system under environment choppiness is implemented using a

wavelength division multiplexing (WDM) method. WDM is employed to increase signal strength using optical amplifiers, resulting in a better signal to noise ratio at the receiver. A WDM OWC system based on hybrid optical amplifier configurations is suggested, which offers a viable option for low-cost and high-efficiency systems.

The simulation is done on Opti system 7.0 software. The software is used to compare the results of DCF technology for pre, post, and balanced fibre arrangement with and without cascaded FBGs at a rate of 10 Gbps on a 120 km SMF and to enhance the Q—factor and reduce the BER of WDM OWC system under rain and dust.

The benefits of high Q-factor and less BER achieved using OWC are further experimented by using modulation techniques like amplitude shift keying (ASK) and physical shift keying (PSK). This also removes complexity of using free space optics (FSO) in the channel. EDFA amplifiers are also used and a comparison study is conducted to determine which modulation technique is more effective for communication. This part of the research examines the performance of an OWC system based on ASK and PSK modulation techniques by varying OWC parameters under various atmospheric conditions such as rain, mist, haze, and snow. Finally, the simulation results are discussed and analysed.

CONTENTS

Candidate's Declaration	i
Certificate	ii
Acknowledgement	iii
Abstract	iv
Contents	vi
List of Figures	viii
List of Tables	xii
List of abbreviations	xiii
CHAPTER 1: INTRODUCTION	1
CHAPTER 2: LITERATURE REVIEW	6
CHAPTER 3: DISPERSION COMPENSATION TECHNIQUES	10
3.1: MATHEMATICAL ANALYSIS FOR DCF AND FBG	11
3.2: DIFFERENT CONFIGURATIONS OF DCF	12
3.2.1: PRE-DCF TECHNIQUE	12
3.2.2: POST-DCF TECHNIQUE	13
3.2.3: BALANCED-DCF TECHNIQUE	14
3.3: CIRCUIT MODELS AND SIMULATION	14
3.3.1 OPTI SYSTEM 7.0	19
3.3.2 SIMULATION MODELS WITHOUT CASCADED FBGS	12

3.4: DISPERSION COMPENSATION WITH WDM	33
3.5: RESULTS AND DISCUSSION OF DISPERSION COMPENSATED MODEL	38
CHAPTER 4: WDM OWC SYSTEM ANALYSIS	40
4.1: WDM OWC SYSTEM SIMULATIONS	44
4.2: RESULTS FOR WDM OWC SYSTEM UNDER DIFFERENT WEATHER CONDITIONS	44
CHAPTER 5: SYSTEM ARCHITECTURE OF ASK AND PSK MODULATION TECHNIQUES	45
5.1. ASK MODULATION TECHNIQUE WITH HOAS	46
5.2. PSK MODULATION TECHNIQUE WITH HOAS	46
5.3: OWC DESIGN SIMULATIONS	47
5.3.1: ASK MODULATED OWC DESIGN SIMULATION	48
5.3.2: PSK MODULATED OWC DESIGN SIMULATION	53
5.4: RESULTS FOR DLF BASED MODULATION TECHNIQUES USING OWC CHANNEL AND AMPLIFIERS	53
CHAPTER 6: CONCLUSION AND FUTURE SCOPE	53
6.1: CONCLUSION OF RESEARCH FOR DISPERSION COMPENSATION	53
6.2: CONCLUSION OF RESEARCH FOR WDM OWC CHANNEL WITH EDFA HYBRID CONFIGURATION	53
6.3: CONCLUSION OF RESEARCH ON “ENHANCEMENT OF COUPLER- BASED DELAY LINE FILTERS MODULATION TECHNIQUES USING OPTICAL WIRELESS CHANNEL AND AMPLIFIERS AT 100 GBIT/S”	54
REFERENCES	56
LIST OF PUBLICATIONS	62

LIST OF FIGURES

Figure 1.1: Principle of dispersion compensation fibre	3
Figure 3.2.1: Pre-DCF technique configuration	12
Figure 3.2.2: Post-DCF technique configuration	12
Figure 3.2.2: Post-DCF technique configuration	13
Figure 3.2.3: Balanced-DCF technique configuration	15
Figure 3.3.2.1. Simulation of: (a) pre-DCF model, (b) post-DCF model (c) balanced-DCF model	16
Figure 3.3.2.2. Simulation of amplitude modulation system: (a) pre-DCF technique, (b) post-DCF technique (c) balanced-DCF technique	18
Figure 3.3.2.3. Simulation of: (a) pre-DCF model with cascaded FBGs, (b) post-DCF model with cascaded FBGs, (c) balanced-DCF model with cascaded FBGs	19
Figure 3.3.2.4. Simulation of amplitude modulated: (a) pre-DCF model with cascaded FBGs, (b) post-DCF model with cascaded FBGs, (c) balanced-DCF model with cascaded FBGs	20
Figure 3.4.1. Cascaded FBG and DCF model with WDMs for multiple users	22
Figure 3.5.1. Comparative Q-factor plot of: (a) pre-DCF model with and without using cascaded FBGs, (b) post- DCF model with and without using cascaded FBGs, (c) balanced-DCF model with and without using cascaded FBGs	23
Figure 3.5.2: Comparative bit error plot of: (a) pre-DCF model with and without using cascaded FBGs, (b) post-DCF model with and without using cascaded FBGs,	

(c) balanced-DCF model with and without using cascaded FBGs	24
Figure 3.5.3. Q-factor of cascaded FBGs with WDM mux and de-mux for three users	25
Figure 3.5.4. Eye diagrams of cascaded FBGs and DCF with WDMs for: (a) user-1 at 193.1 THz of wavelength, (b) user-2 at 193.2 THz of wavelength, (c) user-3 at 193.3 THz of wavelength	26
Figure 3.5.5. Post-DCF with cascaded FBG and WDM model: (a) coding at transmitter, (b) decoding at receiver	26
Figure 3.5.6. Comparative Q-factor plot of pre, post and balanced-DCF model with and without using cascaded FBGs	28
Figure 3.5.7 Comparative bit error plot of pre, post and balanced-DCF model with and without using cascaded FBGs at 1550nm	29
Figure 3.5.8: Eye-statures showing Q-factor and BER of different DCF techniques without cascaded FBGs for (a) pre-DCF, (b) post-DCF and (c) balanced-DCF	30
Figure 3.5.9: Eye-statures showing Q-factor and BER of different DCF techniques with cascaded FBGs for (a) pre-DCF, (b) post-DCF and (c) balanced-DCF	31
Figure 3.5.10: Decoded data on oscilloscope visualizer without and with cascaded FBGs for (a) pre-DCF, (b) post-DCF, and (c) balanced-DCF	32
Figure 3.5.11: Comparative plot of average Q-factor of DCF techniques for amplitude modulation with WDM mux and de-mux at 2.5 Gbps for three users with and without using cascading FBGs	35

Figure 4.1: WDM OWC setup illustration	33
Figure 4.2: Attenuation versus visibility plot for dust	35
Figure 4.3: Attenuation versus visibility range plot for rain	37
Figure 4.4: Rainfall rate versus attenuation plot for rain	37
Figure 4.1.1: System config. I simulation using three optical amplifiers	38
Figure 4.1.2: System config. II simulation using two optical amplifiers	39
Figure 4.1.3: Simulation of hybrid configuration of the system	39
Figure 4.2.1: Q-factor plot of Dust at 2.5 Gbps (a) against attenuation (b) against visibility range	41
Figure 4.2.2: Eye-diagram plot of dusty weather for: (a) System config.-I (b) System config.-II (c) Hybrid System config	41
Figure 4.2.3: Q-factor versus visibility range plot for Rain at 2.5 Gbps	42
Figure 4.2.4: Eye-diagram plot of rainy weather for: (a) System config.-I (b) System config.-II (c) Hybrid System config	42
Figure 5.1.1: ASK modulated OWC system using HOAs	44
Figure 5.2.2: PSK modulated OWC system using HOAs	45
Figure 5.3.1. Simulation of HOAs based ASK modulated OWC system	47
Figure 5.3.2. Simulation of HOAs based PSK modulated OWC system	48

Figure 5.4.1. Eye-diagrams for HOAs based ASK OWC system under (a) Haze, (b) Snow, (c) Rain and mist, (d) Medium fog condition 51

Figure 5.4.2. Eye-diagrams for HOAs based PSK OWC system under (a) Haze, (b) Snow, (c) Rain and mist, (d) Medium fog condition 52

LIST OF TABLES

Table 3.3.2.1: Simulation specifications	17
Table 3.5.1: Observation table for Average Q-factor of DCF techniques with and without cascaded FBGs	22
Table 3.5.2: Observation table for average BER (logarithmic) of DCF techniques with and without cascaded FBGs	24
Table 3.5.3: Observation table for Q-factor of DCF techniques with and without cascaded	27
Table 3.5.4: Observation table for average BER (logarithmic) of DCF techniques with and without cascaded FBGs	28
Table 4.1: Variation in attenuation with visibility for Dust	35
Table 4.2: Observation of yearly rainfall rate, range and attenuation for rainy weather in Jaipur city	36
Table 5.4.1: Atmospheric parameters under different climate for free space optics communication	49
Table 5.4.2: Output for Haze condition	49
Table 5.4.3: Output for rain and mist condition	49
Table 5.4.4: Output for snow condition	50
Table 5.4.5: Output for medium fog condition	50

LIST OF ABBREVIATIONS

DCF: dispersion compensation fiber

FBG: fiber Bragg grating

WDM: wavelength division multiplexer

FSO: free space optics

OWC: optical wireless communication

Q-factor: quality factor

BER: -bit error rate

PRBS: pseudo random bit sequence

CW laser: continuous wave laser

MZM: Mach Zehnder modulator

MUX: multiplexers

DE-MUX: demultiplexers

ASK: amplitude shift keying

PSK: phase shift keying

HOAs: hybrid optical amplifiers

CHAPTER-1

INTRODUCTION

The development of the global telephone network in the 20th century has led to many developments in communication systems. Use coaxial cables instead of corrugated cables for high performance. The first coaxial cable connector, used in 1940, was a 3 MHz system capable of carrying 300 audio channels (or a single television channel). The bandwidth of these systems is limited by cable loss which increases at frequencies above 10 MHz

These constraints prompted the creation of microwave communications that use wave power at frequencies between 1 and 10 GHz. In 1950, scientists rediscovered optics to provide solutions to improve communication skills. Optical fibre was invented in the 1960s and has been used to make gastroscopes and other devices that require fibre shortening. The concept of using glass fibre for optical communication is changing as optical fibre can carry light in the same way as trapping electrons in copper wire. Therefore, the fibres can be used in the same way that they are used every day for like electric wires.

Performance of any optical communication system can become better by removing the dispersion from it. The consequence of chromatic dispersion over the execution of an optical fibre system is called inter-symbol interference (ISI). In ISI, pulse spreading takes place, due to which pulses at the output overlap with each other [1]. To reduce the dispersion, dispersion compensation techniques are adopted. Some trending techniques are dispersion compensating fibres (DCF) and Fibre Bragg gratings (FBG) [1]. DCF is used to compensate the dispersion loss caused by single-mode fibre (SMF). Moreover, DCF also attains negative dispersion that makes it special kind of fibre.

Depending on the location of the SMF and DCF, three compensation configurations are available: Pre-DCF, Post-DCF, and Balanced DCF. In pre-DCF, DCF is activated before SMF. For post DCF, DCF is switched after SMF, and for balanced DCF, DCF is activated before and after SMF.

Another Versatile approach for dispersion compensation is Fibre Bragg grating (FBG) [2]. It is a miniature piece of optical fibre. It has a small refractive index in its core. For a uniform FBG, the spacing of these indices is equal, while for a chirped FBG (CFBG), the spacing of these indices is not equal. Uniform FBG also reflects one wavelength of given bandwidth, $\Delta\lambda$, and allows to pass all other wavelengths [2]. The wavelength which gets reflected is called as Bragg wavelength. Chirped FBGs reflect more wavelengths unequally from different places of the core due to which it reduces dispersion.

In this paper, dispersion compensation schemes are studied using four uniform cascaded FBGs at the transmitter side. Transmitter and receiver are connected with three different schemes of DCF. CFGBs are used at the output to compensate the accumulated dispersion over the fibre. Comparative results are presented with and without cascaded FBGs. The analysis of the model is in respect of bit error rate and quality(Q)-factor. Wavelength range of cascaded FBGs are changed according to the user defined parameters. Results are shown for 193 THz range of frequency. Gain of erbium-doped fibre amplifier (EDFA) is 20 dB with noise figure (NF) of 2 dB. The bit rate of the system is set at 10 Gbps. The length of SMF is taken as 120 km and length of DCF is 24 km. The parameter for dispersion in SMF is 16.75 ps/nm/km and parameter for dispersion in DCF is -80 ps/nm/km. Principle of dispersion compensation is shown in figure 1.1, this presents that the addition of positive and negative dispersion decreases the overall impact of dispersion in the system [1].

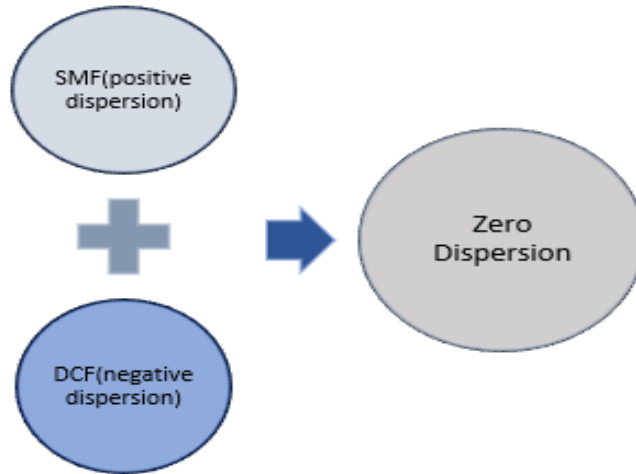


Figure 1.1: Principle of dispersion compensation fibre

This research work is organized into different chapters. Chapter 2 discusses the dispersion compensation techniques. Chapter 3 shows the simulated models of different techniques of DCF with and without using Cascaded FBGs. Comparative simulation results are shown in different plots in chapter 4.

On the other hand, optical wireless communication (OWC) is a telecommunications and computer networking technique that enables a free-space line of sight (LOS) path to transmit information between two points [15]. The OWC is based on optical communication, however, unlike an optical fibre cable or an optical transmission line, it does not use solids as a transmission medium. When a physical connection is not conceivable due to cost or other factors, OWC is generally used [16]. Since this technique enables atmosphere as a form of media of transmission, it is inherently vulnerable to atmospheric phenomena. These interruptions will have a substantial effect on OWC transmission performance. The turbulence in the surrounding environment will cause a rapid fluctuation in received power, lowering the system's quality.

Furthermore, the interruption due to beam of laser will disrupt the transmission intensity in communication, which can be enhanced by the use of an amplifier [17].

Free space optical (FSO) communication is becoming more popular as the demand for high-speed communication systems grows. Optical wireless communication uses lasers as a carrier signal to provide ultra-high-speed and large-capacity communication. Optical wireless communication is prioritized over radio frequency (RF) communication, because it has a narrower beamwidth through the use of lasers, as well as many other advantages such as decreasing the size of the antenna, lowering the power used for the communication system, and providing a higher data rate.

The elements that result in signal attenuation are minimized by utilizing various novel approaches as OWC is a fastest growing field, because of its vast range of applications. Wavelength division multiplexing (WDM) deployment is one example of such a strategy. Optical amplifiers are another option. Combining both of these strategies can be beneficial to the OWC system [22]. According to the International Electrotechnical Commission Standard [27], eye safety regulations limit the maximum permissible emitted power at the transmitter (e.g., below 10 dBm for 1550 nm). Therefore, when using the OWC channel, the transmitted power is set to 9dBm. Using the suggested model, we expand our work in to examine OWC channel under dust storm and rainy weather conditions.

Under dusty and wet weather circumstances, this paper compares two systems that differ in the configuration (config.) of optical amplifiers in WDM systems. Chapter 7 includes the analysis of WDM OWC system under dusty and rainy weather conditions. Chapter 8 includes the simulation models using optical amplifiers for the attenuation and visibility range for dust and yearly rainy weather condition of Jaipur city.

Chapter 9 contains the research findings and discussion.

For many years, optical fibers have been used to meet this demand. However, one disadvantage of these fibers is that they are not suitable for deployment in remote areas, which increases the system's cost. Previously, free-space optics (FSO) appeared to be the most efficient option in various weather turbulence. The research should be focused on more robust technology that can work effectively in choppy environments, and optical wireless communication (OWC) can be proven to be a viable option in this regard.

Excess gain of up to 40 to 50 dB with a low noise figure of 3-5 dB is among the benefits of EDFA. The pump power of this inline amplifier is high, and the gain stability is good. EDFA has low crosstalk in addition to high gain characteristics. The use of EDFA amplifiers in a hybrid configuration can significantly improve system performance [33]. The third research work will examine the OWC channel in the rain, fog, mist, haze, and snow weather conditions using the proposed model.

The system architecture for ASK and PSK modulation techniques is covered in chapter 10. The simulation setup for ASK and PSK modulated OWC design using a hybrid configuration of optical amplifiers (HOAs) is included in chapter 11. Furthermore, with reference to previous research, a comparative analysis is presented under various weather conditions. The conclusion of the research work is covered in chapter 12. Chapter 13 covers the research work's conclusion.

CHAPTER-2

LITERATURE REVIEW

Different research papers are studied on dispersion compensation fibres, fibre Bragg gratings, FSO under dust, visibility range in different weathers, WDM FSO using optical amplifiers. Many researchers have designed models to reduce the dispersion from the transmitted signal through fibre optic. This chapter includes the literature review of all the research papers that are useful in reducing the dispersion from the transmitted signal, to design a free space communication system using OWC channel, and to enhance the signal quality while using modulation techniques using OWC channel approach in environmental conditions.

1. First, in research data, using DCF and FBG as the scattering charge method can improve the system's overall performance. In this article, DCF and FBG, which are dispersion compensators, were compared by comparing the Q factor and 100 Gbps BER of SMF at 120 km using Opti system 7.0 software. Therefore, we recommend using DCF as the best way for compensating for chromatic dispersion in pre-compensation mode [1].
2. In the second study, cascaded fibre Bragg grating (FBG) are introduced to decrease the dispersion of optical signals in a single type of optical fibre. This in turn improves performance, as observed by a slight error rate (BER) and a positive factor (Q factor). The design consists of four equal parts of FBG connected to the transmitter to receive the narrow linewidth ($\Delta\lambda$) of the optical signal, that is the main delay. Optisystem7 makes it possible to simulate a prototype in a WDM system with or without a prototype over a distance of 200 km.

The criteria that did not show a 12% improvement in performance were examined, including visual imaging, Q factor, and BER [2].

3. Optical signals are distorted as they travel along with a fibre optic transmission system. This is one of the most critical issues in fibre optic transmission, usually due to dispersion. In a third research paper, the wavelength division multiplexing (WDM) method was used to apply the DCF. At different frequencies, this WDM system identifies with and without DCF. The DCF's performance is verified by simulating the results of parameters such as quality, eye shape, and BER [3].
4. The fourth study presents the use of DCF in DWDM transmission mode and the transfer of light emission energy. A standard DWDM with 200 GHz channel spacing, 300 km optical transmission length and 16 channels of an erbium-doped fibre amplifier (EDFA) was used in the Opti system. Contrasting to functions is consistent with bit rate (BER), Q factor, and gain power for optical power conversion from -4, -2, 0, 2, 4, 6, 8, and 10 dBm at 10 Gbps and 40 Gbps bit rate. The results showed that the 16 channels with DCF at bit rates of 10 Gbps and 40 Gbps in total reduced cracking. The release of optical power had a major impact on the performance of high bit rates [4].
5. At wavelengths near to Bragg resonance, fibre arrays operating in transmission mode will offer considerable dispersion. The net dispersion of the stopbands of two subsequent networks is considerably affected when numerous networks are cascaded for a Wavelength Division Multiplexing (WDM) application. In the fifth study, the distribution of fibre networks is discussed step by step, and apply a classification for the simultaneous payment of the dispersion and dispersion group (GVD) for several methods of experiment in the WDM optical wave system.

We also discuss the advantages of the differences that result from the cascade gate-based add-loss multiplexers [5].

6. A traveling-wave semiconductor optical amplifier is a useful device for eliminating the effect of fog on free-space optical communication links. With the presence of this efficient device, multiple TX/RX system architectures are capable of improving performance under fog atmospheric effect by ensuring higher received power and lower bit error rate. The study employs a simulation tool Opti system 7 to implement the architecture of a multiple TX/RX system with a traveling wave semiconductor optical amplifier under fog atmospheric conditions [15].
7. The aerial FSO communication system has been thoroughly discussed, from its fundamentals to error performance using OOK, PPM modulation schemes. The atmospheric channel's properties have also been illustrated in terms of transmission loss and scintillation [16].
8. Due to the multiple benefits, it provides, FSO is advancing in a variety of fields. Several parameters have been enhanced, and steps are being taken to make the system more cost effective as well as effective. The system, which consists of a hybrid combination of amplifiers, EDFA and SOA, has achieved a data rate of 2.5 Gbps. The proposed WDM FSO system based on hybrid optical amplifiers has been a cost-effective and efficient system [18].
9. The OWC is described and its system performance is characterised in work [17]. Atmospheric effects (attenuation and turbulence), channel models, and connectivity performance parameters such as bit error rate (BER) and path loss in weak turbulence were also investigated and discussed.

The OWC system has been designed and simulated for performance characterization with Subang terrestrial.

10. To predict signal attenuation, a dust storm effect based on a recent empirical model is proposed. The results show that a dust storm has a significant impact on system performance, particularly when there is dense dust and the possibility of maintaining a connection is lost. According to this study, an FSO could play a key role in the next generation of wireless networks, which could span hundreds of metres [19].
11. Because FSO performance can degrade due to adverse weather conditions, efforts are made to achieve peak performance. Using optical amplifiers is one such technique. Optical amplifiers not only improve SNR but also extend the system's range [22].
12. In research paper [35], A new approach for evaluating the behaviour of an ASK and PSK modulation-based FSO system using a coupler-based delay line filter under different climatic conditions has been presented, with a high Q-factor and BER close to 0.

CHAPTER-3

DISPERSION COMPENSATION TECHNIQUES

This chapter describes the mathematical distribution of dispersion compensation fibre (DCF) and fibre Bragg gratings (FBG). Additionally, various DCF configurations (such as pre, post, and balanced) are also discussed here.

3.1: MATHEMATICAL ANALYSIS FOR DCF AND FBG

The generally used fibre for transmission links is common single mode fibre (CSMF). CSMF has a dispersion of 17 ps/nm/km in 1550 nm window [2]. For longer distance of transmission, this dispersion becomes immense due to which it reduces the signal to noise ratio and simultaneously increases bit error rate. So, the main objective with DCF is to induce the negative dispersion in the working range of wavelengths [1]. Induced negative dispersion compensates the positive dispersion and quality of signal improves.

The relationship of dispersion with the second derivative of propagation constant (β) is shown in equation (3.1.1) [1].

$$D = \frac{-2\pi c}{\lambda^2} \frac{d^2\beta}{d\omega^2} = \frac{1}{c} \left(2 \frac{dn_e}{d\omega} + \omega \frac{d^2n_e}{d\omega^2} \right) \quad (3.1.1)$$

Where, c , λ , ω and n_e represents the speed of light in vacuum, wavelength, frequency and index(effective) respectively.

Equation (2) is defining the constant of propagation-

$$\beta = k_o n_e = \frac{\omega}{c} n_e = \frac{2\pi}{\lambda} n_e \quad (3.1.2)$$

Effective index number can be defined as-

$$n_e = \Delta n_e + n_o \quad (3.1.3)$$

Where, Δn_e is representing difference of effective index and

n_o is representing cladding's refractive index.

Now, equation (4) is defining the dispersion as-

$$\begin{aligned} D &= \frac{-2\pi c d^2}{\lambda^2} \frac{k_o \Delta n_e}{d\omega^2} + \frac{-2\pi c d^2}{\lambda^2} \frac{k_o n_o}{d\omega^2} \\ &= D_{waveguide} + D_{material} \end{aligned} \quad (3.1.4)$$

The equation (5) given below is showing the elimination of dispersion [1].

$$D_{TF} L_{TF} + D_{DCF} L_{DCF} = 0 \quad (3.1.5)$$

Where, D_{TF} is coefficient of dispersion for transmission fibre, L_{TF} is representing the length of transmission fibre, D_{DCF} is coefficient of dispersion of DCF and L_{DCF} is the length of DCF.

Another discussed technique for dispersion compensation is FBG. These are very flexible in use. FBG can perform single as well as multichannel DCM which are not practical with DCF [1]. FBG has a grid period defined as the distance between two vertices of the refractive index. Narrow spectrum of wavelength λ_B is mirrored by FBGs, while it passes all other wavelengths. Mirrored wavelength is Bragg wavelength shown in equation (6)-

$$\lambda_B = 2\Delta n_g \quad (3.1.6)$$

Where, λ_B is denoting the wavelength(nm) which got reflected, Δ is representing the grating period (nm) and n_g is the refractive index (effective).

3.2: DIFFERENT CONFIGURATIONS OF DCF

There are mainly three configurations of DCF techniques which are described below as:

3.2.1: PRE-DCF TECHNIQUE

In the pre-DCF technique, the DCF fibre is positioned in front of single-mode fibre (SMF) and then the information is transmitted. Due to this placement, the dispersion of the signal gets reduced. The block illustration of this technique is given in the Figure 3.2.1

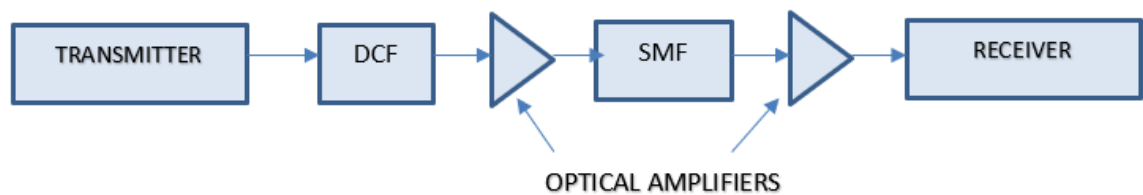


Figure 3.2.1: Pre-DCF technique configuration

3.2.2: POST-DCF TECHNIQUE

In the post-DCF technique, the DCF fibre is placed after the single-mode fibre (SMF) and then the information is transmitted. Due to this placement, dispersion of the signal gets reduced but it is not less as compared to the pre-DCF technique. The block illustration of this technique is given in figure 3.2.2.

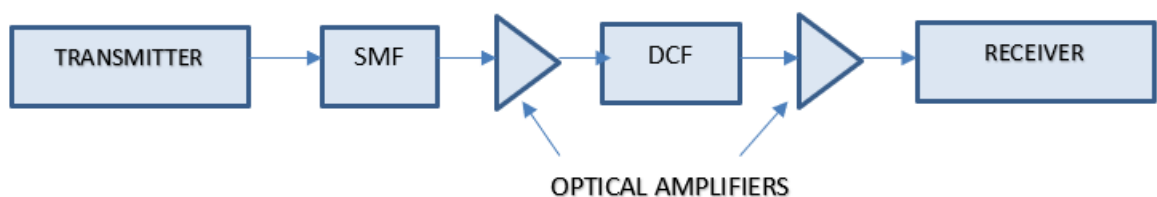


Figure 3.2.2: Post-DCF technique configuration

3.2.3: BALANCED-DCF TECHNIQUE

In the balanced-DCF technique, DCF fibre is placed on both the sides of SMF or pre-DCF and post-DCF are combined together. Due to this technique, the dispersion of the signal gets reduced more than the single pre-DCF and post-DCF technique. The block illustration of this technique is given in the figure 3.2.3.

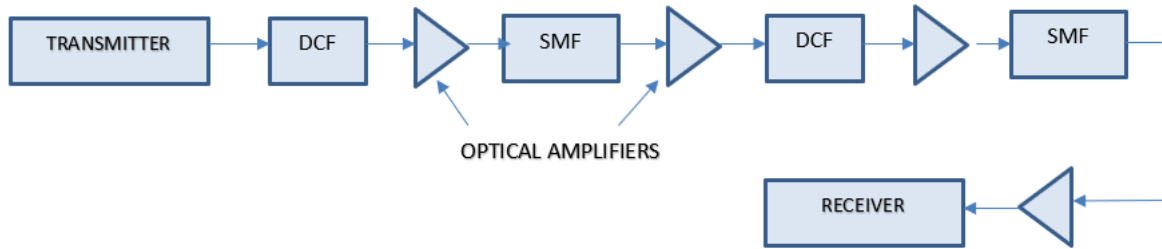


Figure 3.2.3: Balanced-DCF technique configuration

Equations 3.1.1 to 3.1.6 are covering the mathematical analysis of DCF and FBG in section 3.1. Different configurations of DCF and their block illustration are presented in section 3.2.

3.3. CIRCUIT MODELS AND SIMULATION

First released in 2000, Opti System is a fast and robust new software development tool. Users may plan, test, and replicate their ideas with this tool. as many visual combinations of processes as possible. As the discussion progresses, so do software development tools. In fact, Opti wave recently added new technologies that streamline communication and device control. These add-ons allow users to run experiments remotely and use Opti System’s extensive library of visual aids and photonic devices to create objects lost in their experimental setup, thereby eliminating the need for users to use materials. essential. Users can also modify the experience with simulation results during design.

Opti System's simulated environment has found a niche in education and training, giving these schools the opportunity to study optical network without the need for luxuries. This is particularly useful for teaching students about optical connectivity and for introducing new network professionals to various network design systems supported by Opti System. Opti System's wide selection of applications means that each of its users can hone their skills in a variety of optical configurations, resulting in better workforce planning.

This chapter discusses the simulation models performed on Opti system 7.0. The configurations of DCF which have been discussed in chapter 3 are shown here with cascaded FBGs and without cascaded FBGs.

3.3.1: OPTI SYSTEM 7.0

In an industry where cost-effectiveness and efficiency are critical to success, the award-winning Opti system can reduce the time and cost of developing optical systems, connections and components [9].

Opti System is a cutting-edge, quickly expanding, and a robust software development tool that allows users to plan, test, and simulate software virtually any kind of optical connection in the stratum of transmission of a diverse range of optical networks, including LAN, SAN, MAN, and ultra-long-haul. From the component level, it enables optical communication system design and planning to the levels simultaneously, as well as visual analysis and scenarios [9].

3.3.2: SIMULATIONS

The proposed models of DCF technique are of three types based on the placement of DCF with reference to SMF. These are discussed as pre-DCF, post-DCF and balanced-DCF.

Based on these three discussed techniques, three circuit models are simulated Figure 4.2.1 is representing the simulation models for different compensation techniques.

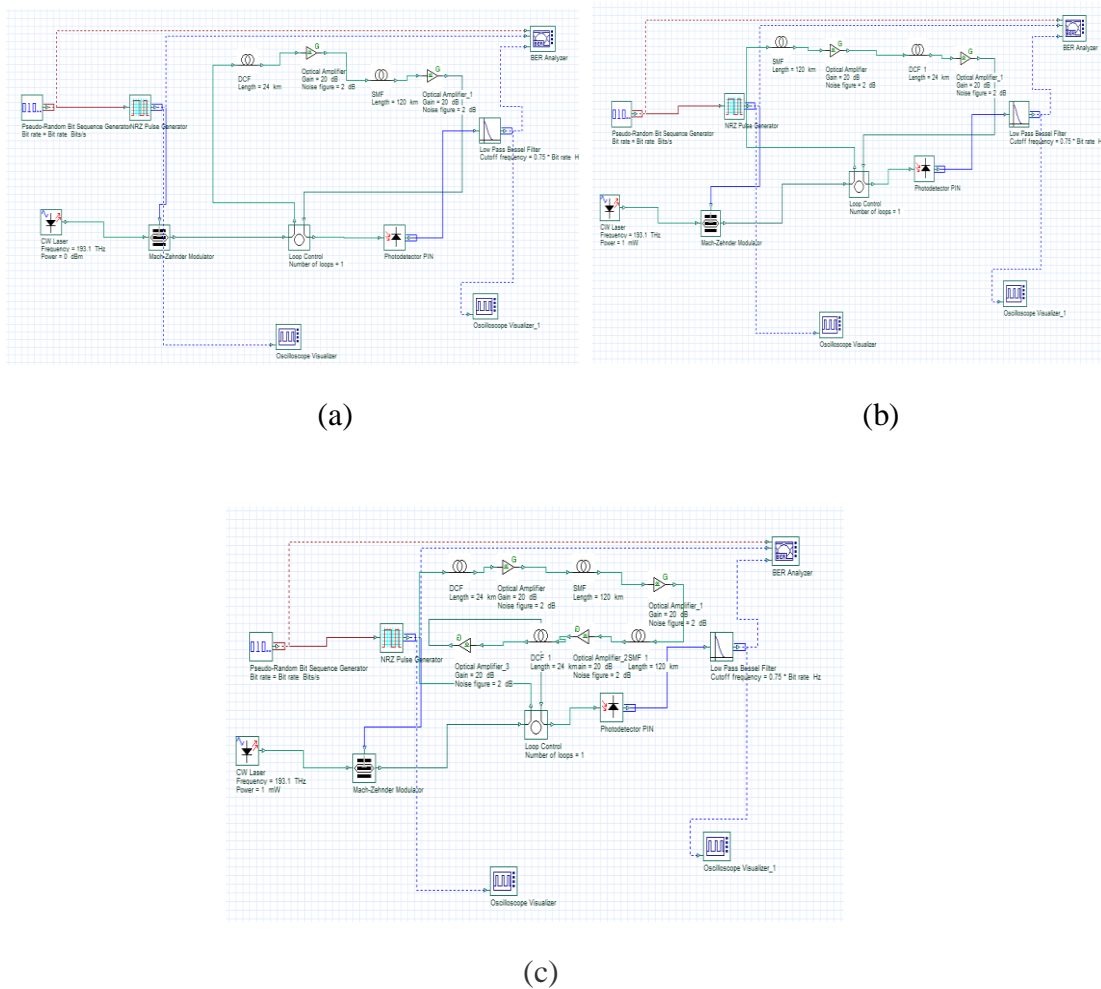


Figure 3.3.2.1. Simulation of: (a) pre-DCF model, (b) post-DCF model (c) balanced-DCF model.

The transmitter part of the system contains pseudo-random bit sequence generator (PRBS), CW laser of 1550nm wavelength, Mach Zehnder modulator (MZM) and non-return-to zero (NRZ) pulse generator. The signal is sent at bit rate of 10 Gbps. The course of the channel consists of SMF of length 120km, DCF of length 24 km and EDFA amplifiers of gain 20 dB. Channel path is connected with the loop control having no. of loops equal to 1, which means signal is getting amplified one time.

Position of DCF is changed with respect to SMF so that all three (pre, post and balanced) techniques of dispersion compensation can be verified.

Receiver section of the system consists of PIN photodetector to transform the optical signal into electrical signal. It is further connected with low pass Bessel filter and bit error analyser to obtain the Q-factor and BER of the signal respectively.

Figure 4.2.2. is representing the simulation models of amplitude modulated signal for different compensation techniques.

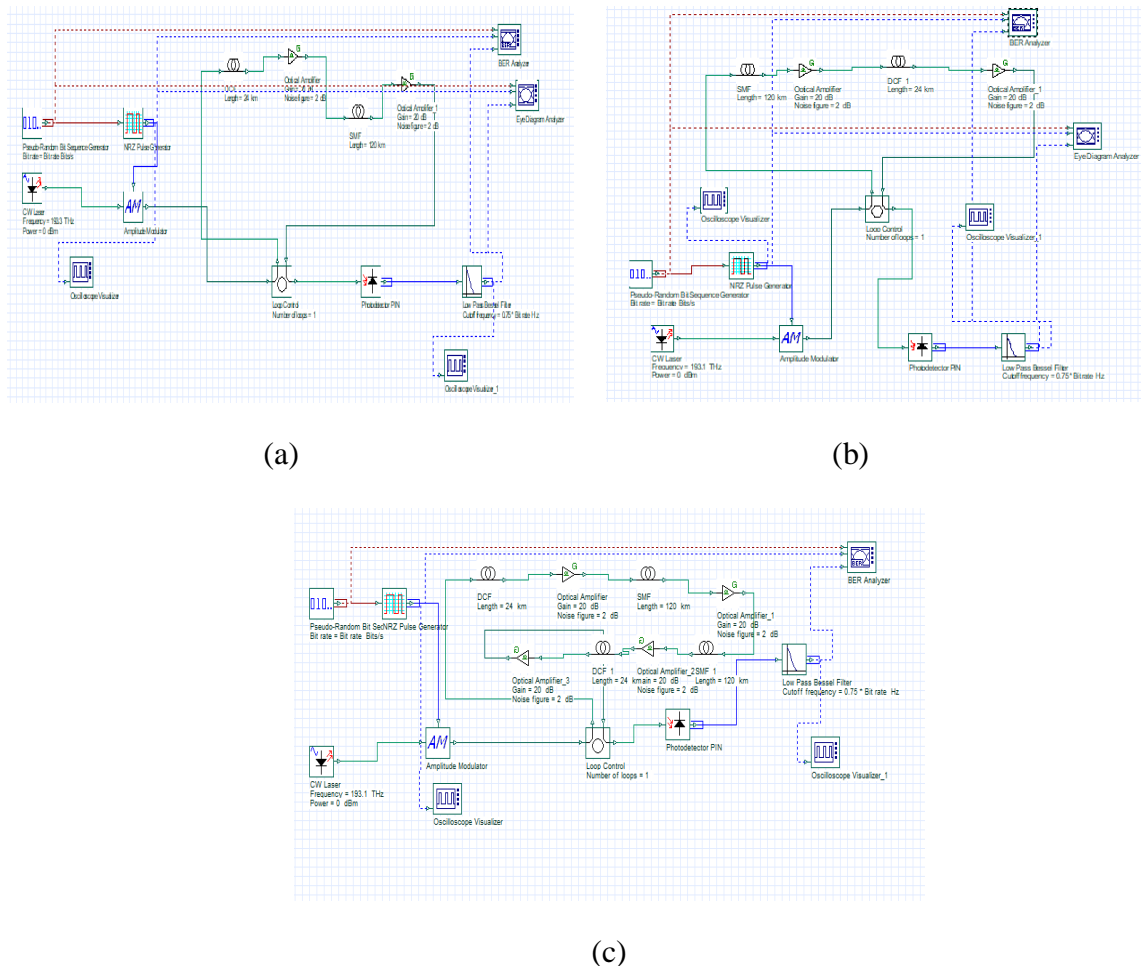


Figure 3.3.2.2. Simulation of amplitude modulation system: (a) pre-DCF technique, (b) post-DCF technique (c) balanced-DCF technique.

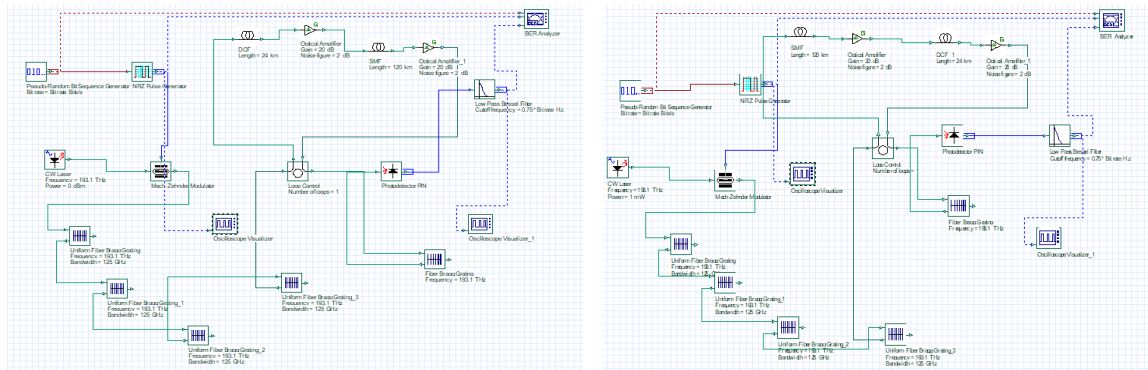
The transmitter part of the system contains a pseudo-random bit sequence generator (PRBS), CW laser of 1550nm wavelength, amplitude modulator (AM), and non-return-to-zero (NRZ) pulse generator. The position of DCF is changed with respect to SMF so that all three techniques of dispersion compensation can be verified. The receiver section of the system consists of a PIN photodetector to transform the optical signal of light into an electrical signal. The specifications used for simulation are shown in Table 3.3.2.1.

Table 3.3.2.1: Simulation specifications

Sr. No.	Parameters	Value
1.	System bit rate (Gbps)	10
2.	Frequency (THz)	193.1
3.	Length of DCF fiber(km)	24
4.	Length of fiber (km)	120
5.	DCF attenuation (dB/km)	0.3
6.	Fiber attenuation (dB/km)	0.2
7.	DCF dispersion(ps/nm/km)	-80
8.	SMF dispersion(ps/nm/km)	16.75

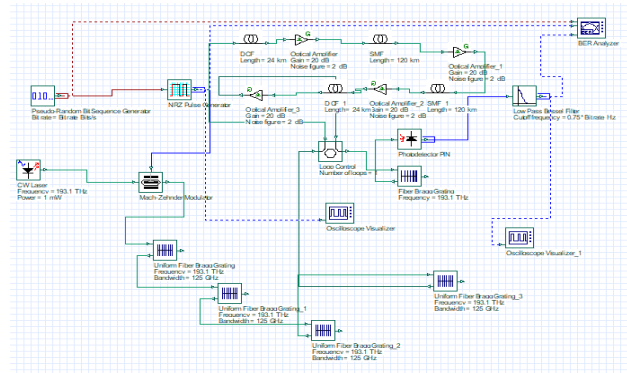
DCF circuit simulations, shown in Figure 3.3.2.1 and 3.3.2.2. are further analysed by introducing cascaded FBGs in each of the three techniques of it. To implement this concept, four cascaded uniform FBGs are connected after MZM of the transmitter part. The wavelength of FBGs and CW laser are matched. Signal is then transmitted to the channel path via loop control.

At the yield of channel path, chirped FBG is connected which is used to eliminate the dispersion existing in the signal. Then the signal travels through the PIN photodetector, low pass Bessel filter and finally observed at BER analyser. Figure 3.3.2.3. is showing simulation models of pre, post and balanced techniques of DCF with cascaded FBG.



(a)

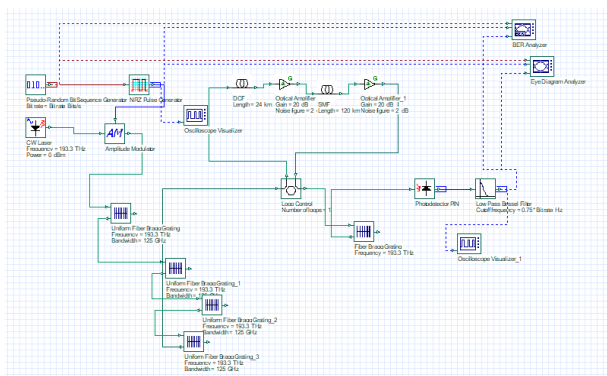
(b)



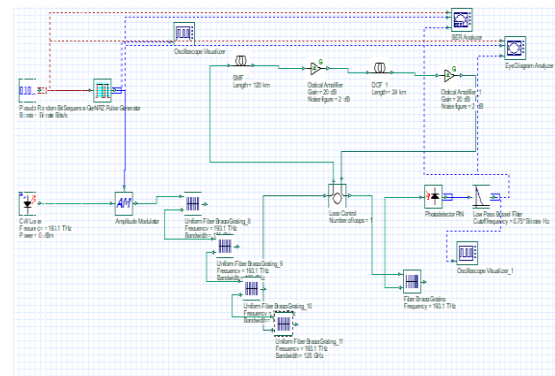
(c)

Figure 3.3.2.3. Simulation of: (a) pre-DCF model with cascaded FBGs, (b) post-DCF model with cascaded FBGs, (c) balanced-DCF model with cascaded FBGs

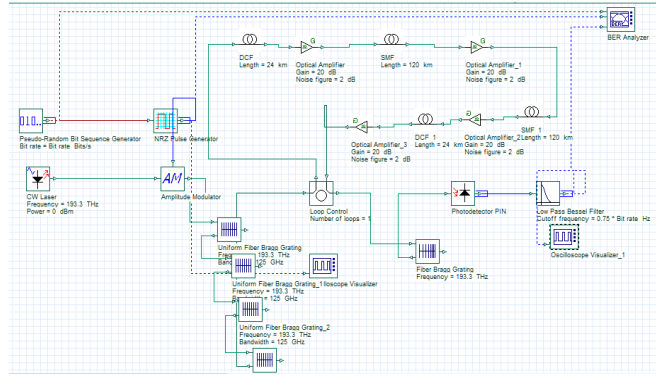
Figure 3.3.2.4. is showing simulation models of pre, post, and balanced techniques of DCF with cascaded FBGs for the amplitude modulated signal.



(a)



(b)



(c)

Figure 3.3.2.4. Simulation of amplitude modulated: (a) pre-DCF model with cascaded FBGs, (b) post-DCF model with cascaded FBGs, (c) balanced-DCF model with cascaded FBGs.

Simulation of different dispersion reducing models with the help of DCF and FBGs are presented. Specific parameters decided during simulation are given in Table 3.3.2.1. Different configurations of DCF (pre, post and balanced) are combined with cascaded FBGs as shown in Figure 3.3.2.3 and 3.3.2.4. The simulation software tool i.e., Opti-system 7.0 is easy to use and readily available on internet.

3.4: DISPERSION COMPENSATION MODEL WITH WDM

WDM systems are popular among telecommunications firms. It increases network capacity without installing extra fibre. Using distinct wavelengths of laser light, the WDM technology in optical communication carries multiple optical carrier messages on a single fibre. The WDM technology achieves bidirectional communication over a single standard fibre with improved capacity. The advantages of WDM include increased capacity, transparency, wavelength reuse, scalability, and dependability.

A basic WDM system consists of a transmitter and a receiving end. At the transmitter end, a number of multiplexers are mounted, each of which multiplexes multiple optical signals onto a single fibre.

To disperse the signal to various users, demultiplexers are inserted at the receiver end. At the receiver, an electrical signal is created by converting an optical signal. via a photo detector. Resulting signal is then distributed to a large number of consumers.

The aforementioned simulation model presents three different compensation schemes that can be implemented using cascaded FBGs. In order to make the system effective for different users at the same time, a wavelength division multiplexer (WDM) and a demultiplexer are required. WDM is easy to implement and also provides higher signal bandwidth.

Different signals of different wavelengths (193 THz range) are multiplexed together and then transmitted through optical links. Due to the different wavelengths, unnecessary signal mixing is avoided, and a demultiplexer is used to distinguish between signals and send them to the appropriate recipients. Figure 3.4.1. shows the system model of WDM multiplexer and demultiplexer with multi-user cascaded FBG and DCF.

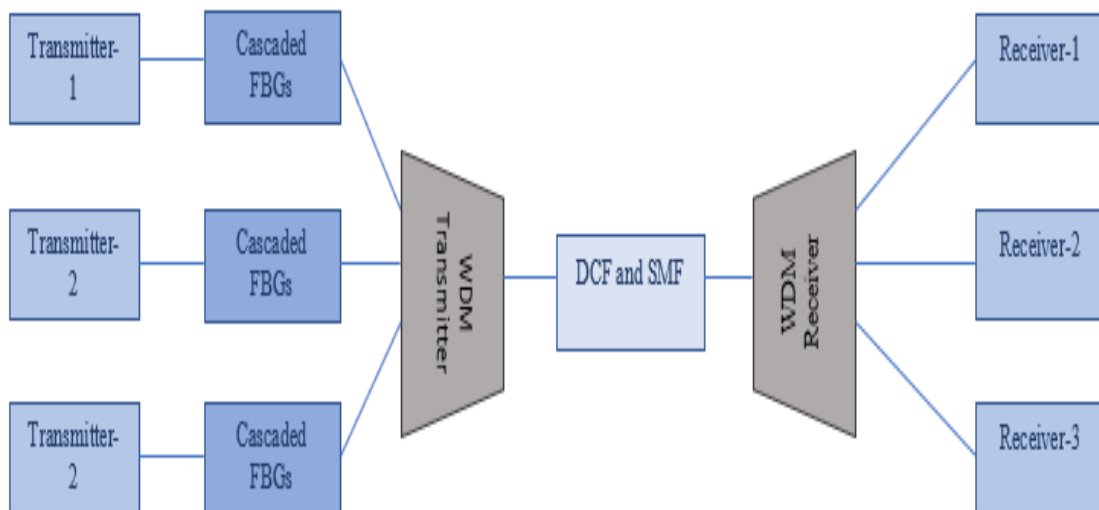


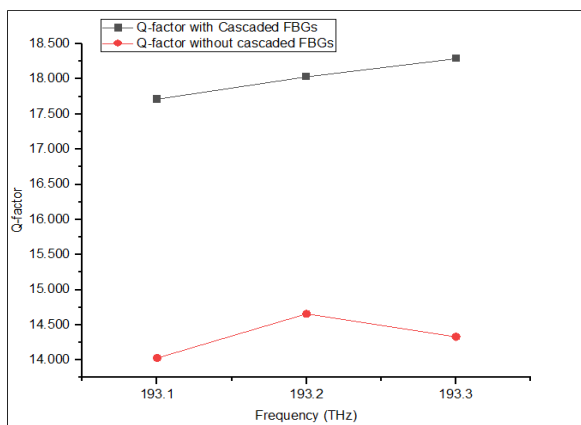
Figure 3.4.1. Cascaded FBG and DCF model with WDMs for multiple users.

Cascaded FBG and dispersion compensation model is shown in Figure 3.4.1. This model comprises WDM so that different transmitters or users can send different wavelengths through a single channel. This model has been simulated with all the mentioned configurations of DCF in section 3.3 and the results of these simulations are presented in next section 3.4.

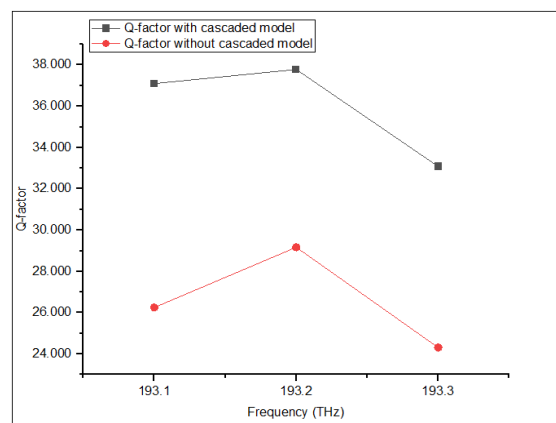
3.5: OUTCOME AND DISCUSSION

This chapter displays the outcomes of simulation models that are presented in section 3.3 and section 3.4. Comparative plots are made for different configurations of DCF with cascaded FBGs and without cascaded FBGs.

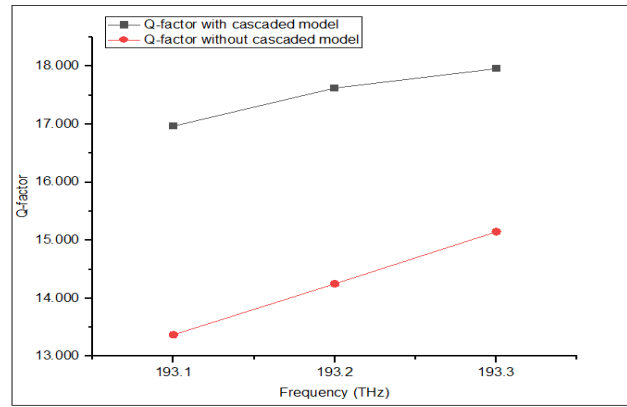
Comparative results are presented for each technique of DCF system shown in Figure 3.5.1. and Figure 3.5.2. at different frequencies. Figure 3.5.1. is showing the comparative Q-factor plot obtained at different frequencies for pre, post and balanced DCF techniques with and without use of cascaded FBGs.



(a)



(b)



(c)

Figure 3.5.1. Comparative Q-factor plot of: (a) pre-DCF model with and without using cascaded FBGs, (b) post- DCF model with and without using cascaded FBGs, (c) balanced-DCF model with and without using cascaded FBGs.

The simulation of pre, post and balanced DCF models shown in Figure 3.3.2.1. are observed at different frequency range of 193 THz. By changing the frequency, slight changes are observed in quality(Q)-factor and bit error rate (BER) of received signal. Similarly, the simulation of pre, post and balanced DCF with cascaded FBG models shown in Figure 3.3.2.3. are also observed at different frequency range of 193 THz. Frequencies of cascaded uniform FBGs and the chirped FBG connected at the yield are changed simultaneously to match with the wavelength of CW laser. Average Q-factor and average BER are then computed for three dissimilar frequencies and based on that, pre, post and balanced compensation techniques of DCF model with and without cascaded FBG are differentiated. The Table 3.5.1 is showing the average Q-factor of DCF techniques with and without using cascaded FBGs.

Table 3.5.1: Observation table for Average Q-factor of DCF techniques with and without cascaded FBGs.

Sr. No.	Technique	Average Q-factor	Average Q-factor with Cascaded FBGs	Percentage improvement (%)
1.	Pre-DCF	14.34	18.011	25.59
2.	Post DCF	26.581	35.987	35.38
3.	Balanced DCF	14.256	17.517	22.87

Figure 3.5.2 is showing the comparative logarithmic plot of BER observed at BER analyser for pre, post and balanced DCF technique with and without cascaded FBGs.

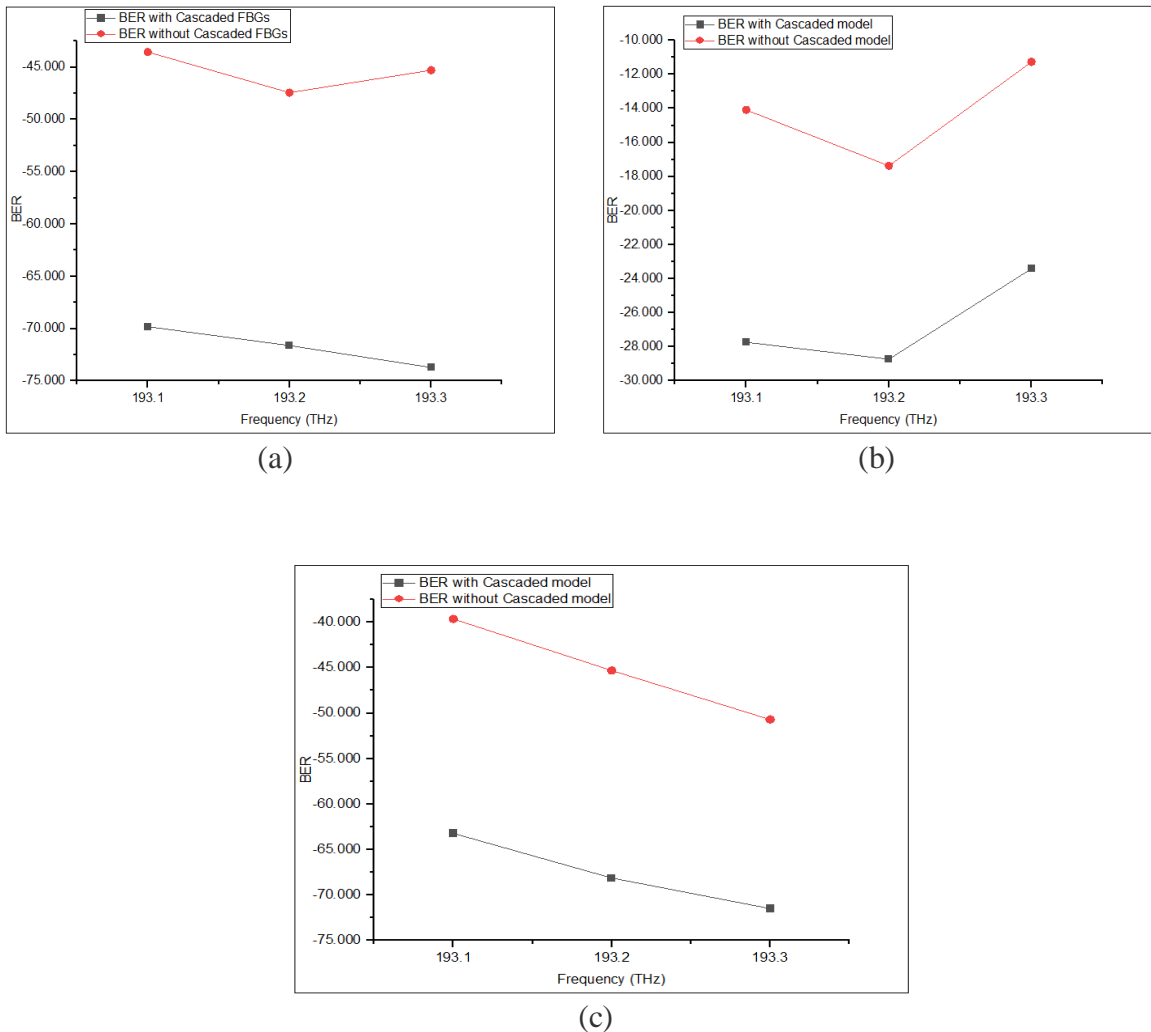


Figure 3.5.2: Comparative bit error plot of: (a) pre-DCF model with and without using cascaded FBGs, (b) post-DCF model with and without using cascaded FBGs, (c) balanced-DCF model with and without using cascaded FBGs.

Average bit error rate is taken for three frequencies in 193 THz range and based on that, pre, post and balanced compensation techniques of DCF model with and without cascaded FBGs are differentiated. The Table 3.5.2 is showing the observations of the BER of DCF techniques with and without cascaded FBGs.

Table 3.5.2: Observation table for average BER (logarithmic) of DCF techniques with and without cascaded FBGs.

Sr. No.	Technique	Average BER (dB)	Average BER (dB) with Cascaded FBGs	Percentage improvement (%)
1.	Pre-DCF	-45.435	-71.707	57.69
2.	Post DCF	-14.248	-26.623	86.85
3.	Balanced DCF	-45.219	-69.325	53.30

As it is evidenced from the Figure 3.5.1. that by introducing a set of cascaded FBGs at the transmitter part, Q-factor of the signal is increased which means there is lower rate of energy loss in the message signal. From Figure 3.5.2, it has been noticed that cascaded FBGs have reduced the bit errors in the signal which means the transmitted bits have not been altered due to noise or distortion. Among all the DCF techniques, the highest percentage change in performance of cascaded FBGs is observed with post-DCF technique. This technique is then studied with WDM mux and de-mux for three different users which mainly is useful for multiple applications. The best Q-factor is obtained at 2.5 Gbps. The Figure 3.5.3 presents the plot of Q-factor with and without cascaded FBGs with WDM.

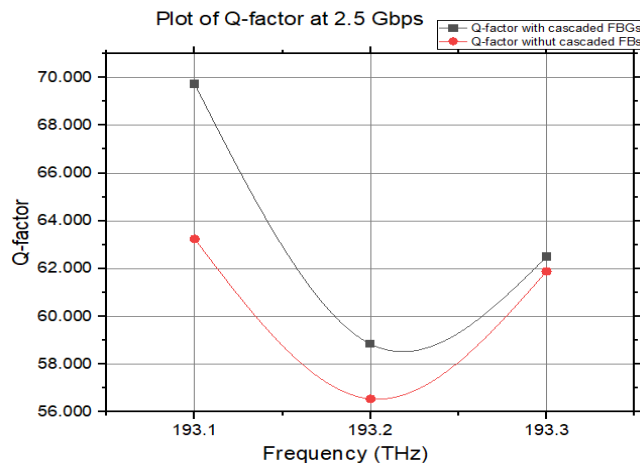


Figure 3.5.3. Q-factor of cascaded FBGs with WDM mux and de-mux for three users.

From Figure 3.5.3 it is observed that post-DCF model provides improved Q-factor for three different users in presence of cascaded FBGs with WDM mux and de-mux. Figure 3.5.4 is showing the eye diagrams for three different users.

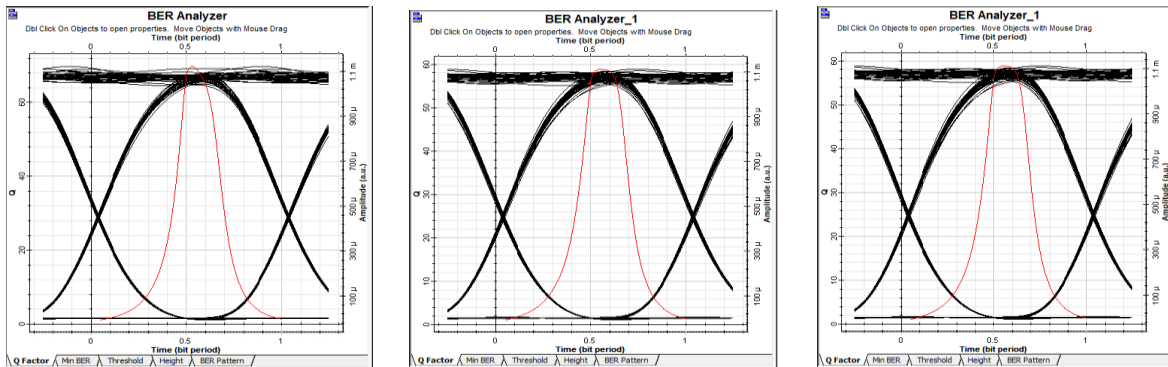
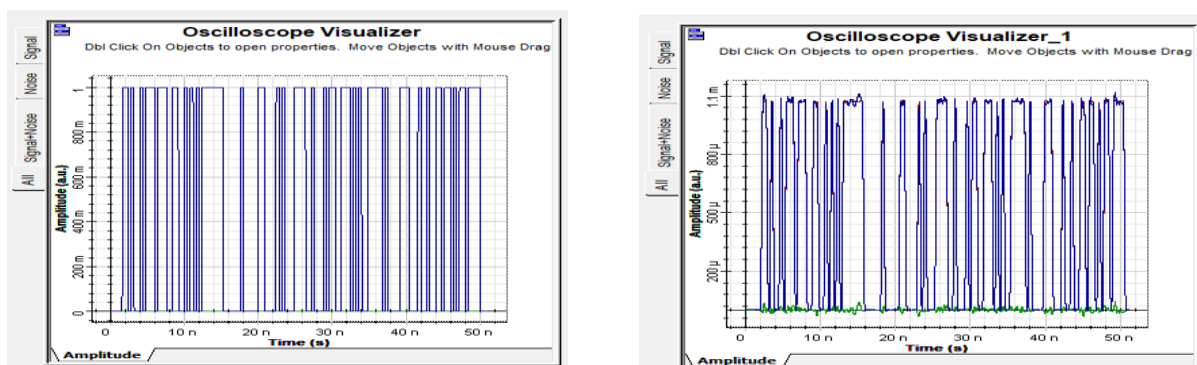


Figure 3.5.4. Eye diagrams of cascaded FBGs and DCF with WDMs for: (a) user-1 at 193.1 THz of wavelength, (b) user-2 at 193.2 THz of wavelength, (c) user-3 at 193.3 THz of wavelength

Figure 3.5.5 is representing the coding and decoding in the post-DCF with cascaded FBG model and WDM at the transmitter and receiver side respectively. These are seen with the help of oscilloscope visualizer connected at transmitter and receiver side. It has been observed that the obtained time span is same at both the sides, so the correct information is retrieved without dispersion.



(a)

(b)

Figure 3.5.5. Post-DCF with cascaded FBG and WDM model: (a) coding at transmitter, (b) decoding at receiver.

The Opti system simulation for reducing dispersion has been implemented successfully. This chapter presented different comparative plots among DCF configurations with cascaded FBGs and without cascaded FBGs. The results are taken relating to Q-factor and bit error rate (BER) and eye-stature. The wider the eye is opened the better is the amount of information received. Oscilloscope visualisers are connected to the system to show the coding and decoding at the transmitter and receiver.

Comparative results are presented for each technique of the DCF system with amplitude modulated signal shown in Figure 3.3.2.2. and Figure 3.3.2.4. at 1550 nm wavelength. Figure 3.5.6 is showing the comparative Q-factor plot obtained at 1550 nm wavelength for pre, post, and balanced DCF techniques with and without the use of cascaded FBGs.

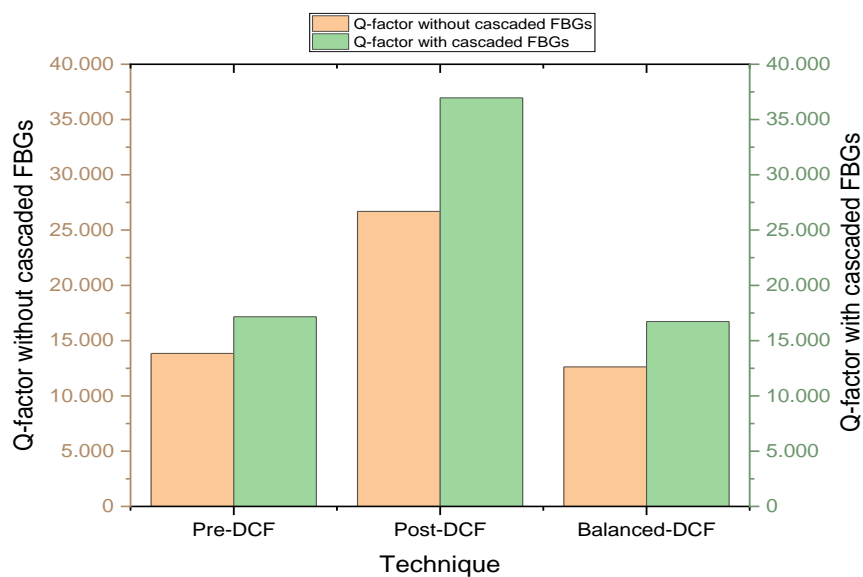


Figure 3.5.6. Comparative Q-factor plot of pre, post and balanced-DCF model with and without using cascaded FBGs.

The simulation of pre, post, and balanced DCF models shown in Figure 3.3.2.3 are observed at 1550 nm of wavelength.

By changing the frequency, slight changes are observed in the quality factor and bit error rate of the received signal. Similarly, the simulation of pre, post, and balanced DCF with cascaded FBG models shown in Figure 3.3.2.4 are also observed at a 1550 nm wavelength. Frequencies of cascaded uniform FBGs and the chirped FBG connected at the yield are changed simultaneously to match with the wavelength of the CW laser.

The quality factor and bit error rate are observed on bit error analyser and based on that, pre, post, and balanced compensation techniques of DCF model with and without cascaded FBG are differentiated.

Table 3.5.3 is showing the Q-factor of DCF techniques with and without using cascaded FBGs.

Table 3.5.3: Observation table for Q-factor of DCF techniques with and without cascaded FBGs at 1550nm.

Sr. No.	Technique	Q-factor without cascaded FBGs	Q-factor with cascaded FBGs	Percentage change
1.	Pre-DCF	13.837	17.159	24%
2.	Post-DCF	26.692	36.961	38%
3.	Balanced-DCF	12.619	16.721	32%

Figure 3.5.7 is showing the comparative logarithmic plot of BER observed at BER analyser for pre, post and balanced DCF technique with and without cascaded FBGs.

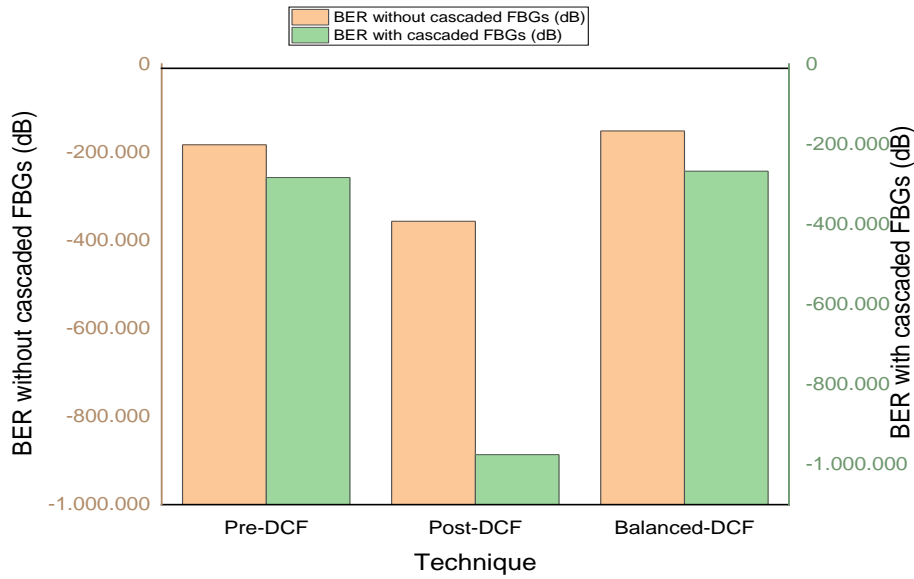


Figure 3.5.7 Comparative bit error plot of pre, post and balanced-DCF model with and without using cascaded FBGs at 1550nm.

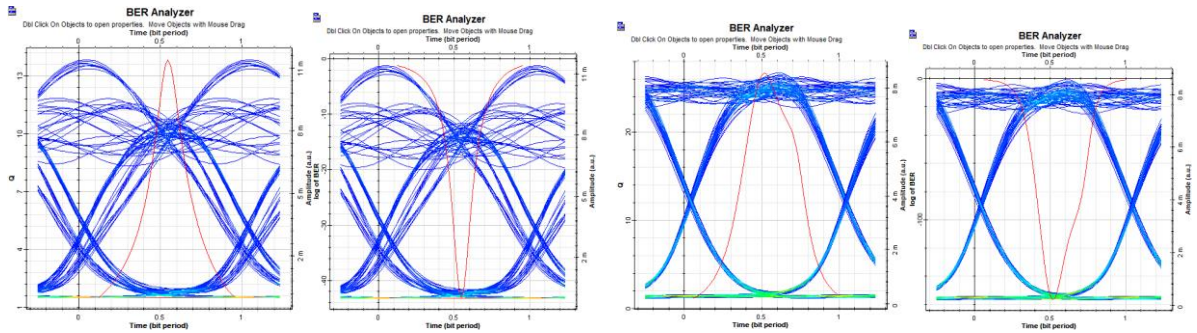
The bit error rate is observed for 1550 nm of wavelength and based on that, pre, post, and balanced compensation techniques of the DCF model with and without cascaded FBGs are differentiated. Table 3.5.4 is showing the observations of the BER of DCF techniques with and without cascaded FBGs.

Table 3.5.4: Observation table for average BER (logarithmic) of DCF techniques with and without cascaded FBGs.

Sr.No.	Technique	BER without cascaded FBGs (dB)	BER with cascaded FBGs (dB)	Percentage change
1.	Pre-DCF	-183.07	-283.46	54%
2.	Post-DCF	≈-356.67	≈-975.187	≈100%
3.	Balanced-DCF	-151.83	-267.58	76%

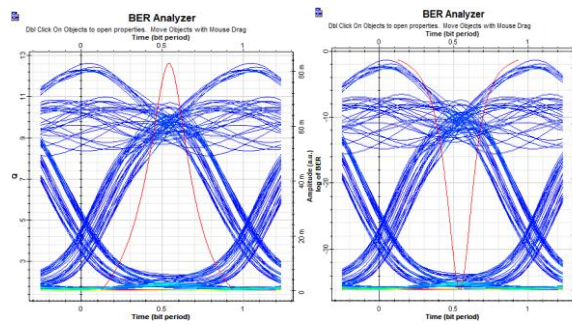
As it can be clearly seen from Figure 3.5.5 that by introducing a set of cascaded FBGs at the transmitter part, the Q-factor of the signal is increased which means there is a lower rate of energy loss in the signal.

From Figure 3.6.6, it is observed that cascaded FBGs have reduced the bit errors in the signal which means the transmitted bits have not been altered due to noise or distortion. Among all the DCF techniques, the highest percentage change in performance of cascaded FBGs is observed with the post-DCF technique. Different eye-statures obtained from the simulations are shown in Figure 3.5.8 and Figure 3.5.9 for without and with cascaded FBGs.



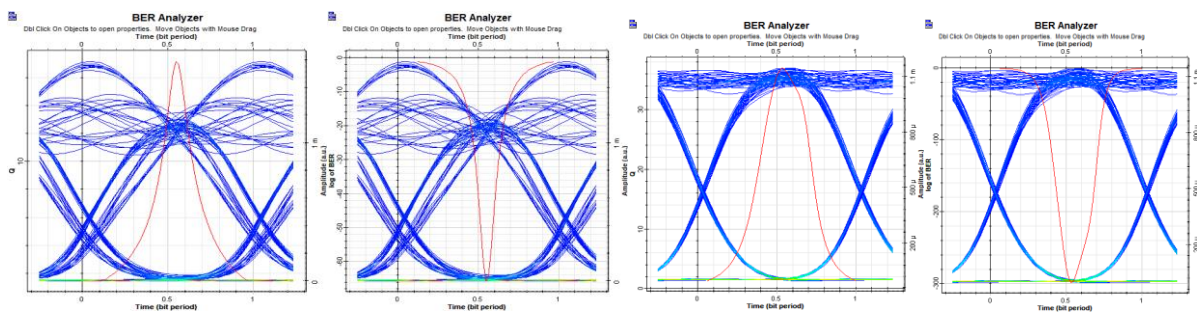
(a) Pre-DCF Q-factor and BER

(b) Post-DCF Q-factor and BER



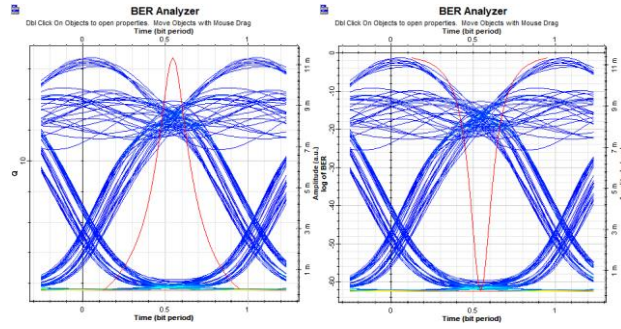
(c) Balanced-DCF Q-factor and BER

Figure 3.5.8: Eye-statures showing Q-factor and BER of different DCF techniques without cascaded FBGs for (a) pre-DCF, (b) post-DCF and (c) balanced-DCF.



(a) Pre-DCF

(b) Post-DCF



(c) **Balanced-DCF**

Figure 3.5.9: Eye-statures showing Q-factor and BER of different DCF techniques with cascaded FBGs for (a) pre-DCF, (b) post-DCF and (c) balanced-DCF.

In the eye-stature of Figure 6.8, the Q-factor and BER have risen as compared to Figure 3.5.9, indicating that the DCF approach with cascaded FBGs delivers better signal than without cascaded FBGs. Through observations of Q-factor, BER and eye-stature, it has been observed that the system is working good with cascaded FBGs instead of non-cascaded FBGs and the major improvements among the DCF techniques are found for post-DCF technique with cascaded FBGs, which is providing the maximum Q-factor, minimum BER and good eye-stature. These results prove that the proposed system for dispersion compensation is suitable to use for optical communication links.

Figure 3.5.10 depicts the decoding of DCF techniques for amplitude modulated signal without and with cascaded FBGs at the transmitter and receiver, respectively, in the WDM model. An oscilloscope visualizer attached to the transmitter and receiver sides is used to observe them. The acquired time span is the same on both sides, indicating that the proper information is retrieved without dispersion.

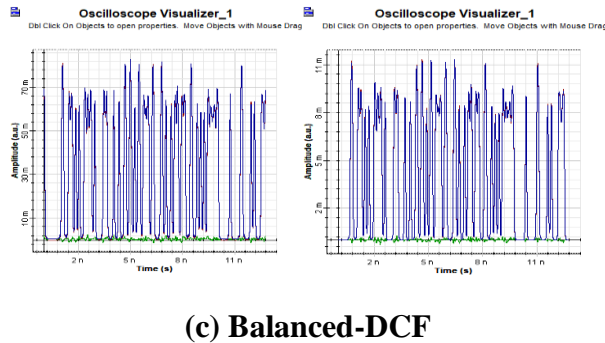
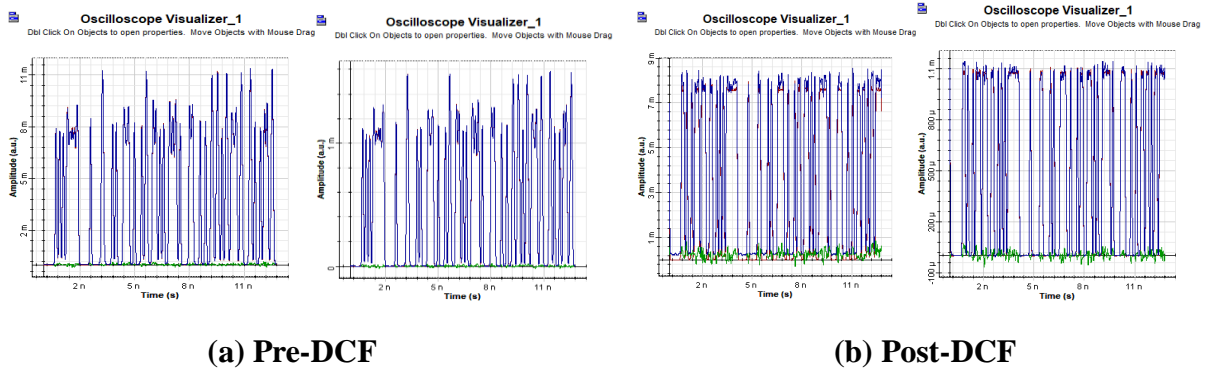


Figure 3.5.10: Decoded data on oscilloscope visualizer without and with cascaded FBGs for (a) pre-DCF, (b) post-DCF, and (c) balanced-DCF.

The notion of amplitude modulation utilizing distinct DCF techniques by employing cascading FBGs is also analysed using WDM mux and de-mux for three separate users, which is primarily helpful for many applications in different wavelength ranges. At 2.5 Gbps, the greatest Q-factor is attained. The plot of Q-factor with and without cascaded FBGs in the WDM model of amplitude modulation is shown in Figure 3.5.11.

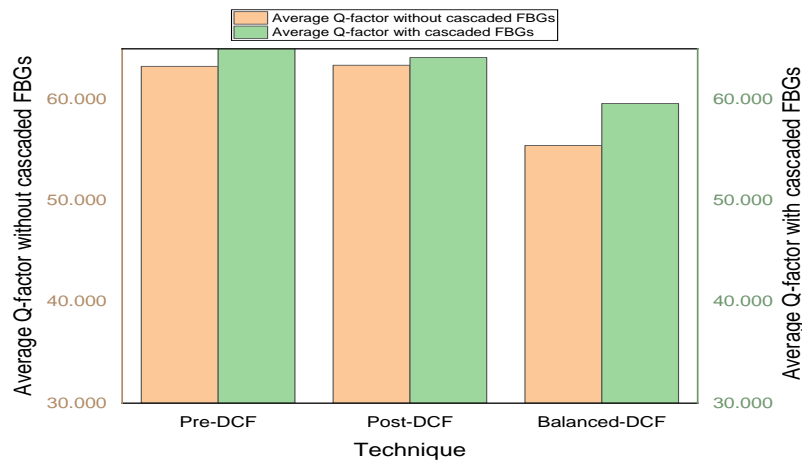


Figure 3.5.11: Comparative plot of average Q-factor of DCF techniques for amplitude modulation with WDM mux and de-mux at 2.5 Gbps for three users with and without using cascading FBGs.

In Figure 3.5.11, the value of Q-factor is computed for three different frequencies ranging from 193.1 THz to 193.3 THz, and the average value is displayed. When cascaded FBGs are used in the WDM system, then the resultant average Q-factor is higher than without cascaded FBGs. At 2.5 Gbps, the obtained BER in the WDM model is zero.

This section 3.5 has shown outcomes of simulations done in section 3.3 for all the DCF configurations with using cascaded FBGs and without using cascaded FBGs. Later the same system has been simulated with amplitude modulator at the transmitter side. After all the simulations, it has been observed that the proposed model utilising cascaded FBGs with DCF technique work best with the post DCF configuration. The percentage change in Q-factor and BER by using post-DCF configuration is highest every time as compared to pre-DCF and balanced-DCF.

CHAPTER-4

WDM OWC SYSTEM ANALYSIS

This chapter analyses the performance of free space optics medium under dust and rainy weather conditions. The yearly rainy weather data is taken specifically for the Jaipur city of Rajasthan. Under both the climatic conditions range and attenuation varies according to the empirical formulas given in equations 4.1, 4.2, and 4.3. The block illustration of the simulated model is given in Figure 4.1.

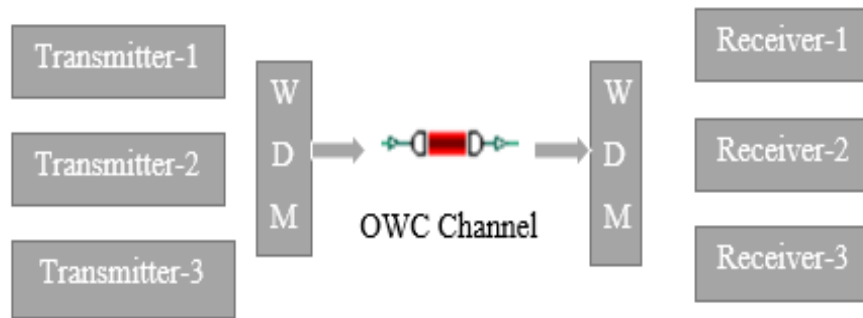


Figure 4.1: WDM OWC setup illustration.

The system is made up of three parts, as shown in Figure 4.1: a transmitter, a transmission medium, and a recipient. The transmitter consists of a pseudo-random bit sequence generator, continuous-wave laser, NRZ pulse generator, and Mach–Zehnder modulator. The receiver has a PIN detector and a Gaussian low pass filter, and the medium of channel is air. Performance is measured using a BER analysers and an optical power meter. The system is evaluated to have the lowest BER at 1550nm, which is the low attenuation window.

The simulated system has made use of a WDM network. The design incorporates optical amplifiers to enhance overall performance and minimize linear and nonlinear effects. An optical amplifier is comprised of a fibre core and an injector signal that activates the

incoming signal. In the layout design, amplifiers can be used in a variety of ways, such as post-amplifiers, pre-amplifiers, and inline amplifiers. The amplifier's position in the system varies in each of these configurations. The need for an amplifier not only helps improve signal strength but also makes it possible to travel even farther. A communication system should be reasonably priced as well as reliable. The fading in the received signal occurs due to different weather conditions which are main cause for power degradation. The analysis of two weather conditions, such as rain and dust are done in this paper.

A. Dust

Dust storms are severe weather events. These are distinguished by high gusts of wind and dusty air over a wide area. Dust storm particles are less than 100 micrometres in size. These can cause severe turbine airflow, limiting clarity to the few miles. The storm's duration can range from a few days to a couple.

The visibility range (V) is the distance over which the transmission drops to 2% of its initial value. Blowing dust or haze is defined as light dust with visibility ranging from 1 km to 10 km. Blowing dust is caused by wind-blown dust, whereas haze is caused by a dust storm that occurs a long distance away from the observation location.

FSO signal attenuation, occurs in dry and semi-dry areas prone to dust storms, is given by eq.

(4.1)-

$$\alpha = 52 \times V^{-1.05} \text{dB/Km} \quad (4.1)$$

Where, V is the visibility in km. Because, it introduces less absorption loss, this model is suitable for 1550 nm, the standard wavelength in optical communications. The changes in attenuation versus visibility range of dust are shown in Figure 4.2. This model is used to examine and analyse the FSO link by considering the Q-factor and BER. The values of the

results attained will be used to evaluate the technology's necessities and constraints. Table 4.1 shows how the attenuation varies with dust visibility range.

Table 4.1: Variation in attenuation with visibility for Dust

V(Km)	Attenuation(dB/km)
5	9.59
10	4.63
15	3.02
20	2.23
30	1.46

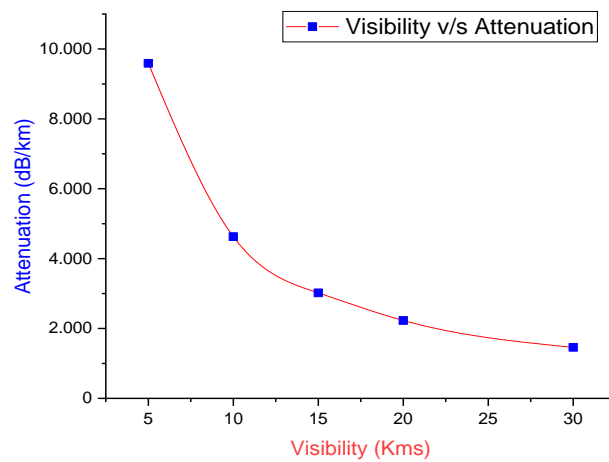


Figure 4.2: Attenuation versus visibility plot for dust

B. Rain

Rain has a significant impact on OWC link. Variation in droplet size frequently causes reflections as well as chromatic aberrations in the atmosphere. The formula of attenuation as a result of rain is given by eq. (4.2)-

$$\alpha = a \cdot R^b \text{ dB/Km} \quad (4.2)$$

The above equation depicts a linear relationship between rainfall rate and attenuation. Here, a and b are frequency-dependent parameters, and R is the rainfall rate in millimetres per hour. Non-selective scattering occurs predominantly because raindrops are larger than the wavelength of the light signal, but Mie scattering can also be used to calculate attenuation values. The specific rain attenuation equation is provided by eq. (4.3)-

$$\alpha_{specific} = 1.076R^{0.67} \text{ dB/Km} \quad (4.3)$$

The above equation denotes specific rain attenuation, and R denotes rate of falling rain in mm/h. [11,12]. The rainfall rate and range data of Jaipur city is taken for different years and based on that attenuation is calculated as shown in Table 4.2, which provides the yearly rainfall rate, range, and attenuation for Jaipur rain conditions. While Figure 4.3 and Figure 4.4 shows the attenuation variation with visibility range and rainfall rate for rain.

Table 4.2: Observation of yearly rainfall rate, range and attenuation for rainy weather in Jaipur city.

Year (Up to 2021)	Rainfall rate(mm/h)	Observed Range (km)	Attenuation(dB/km)	Average Attenuation(dB/km)
2015	213.6	2	39.14	8.55
2016	12.4	10	5.8	
2017	2.8	25	2.14	
2018	0.5	60	0.67	
2019	17.2	5	7.23	

2020	3.4	20	2.44	
2021	3.5	20	2.49	

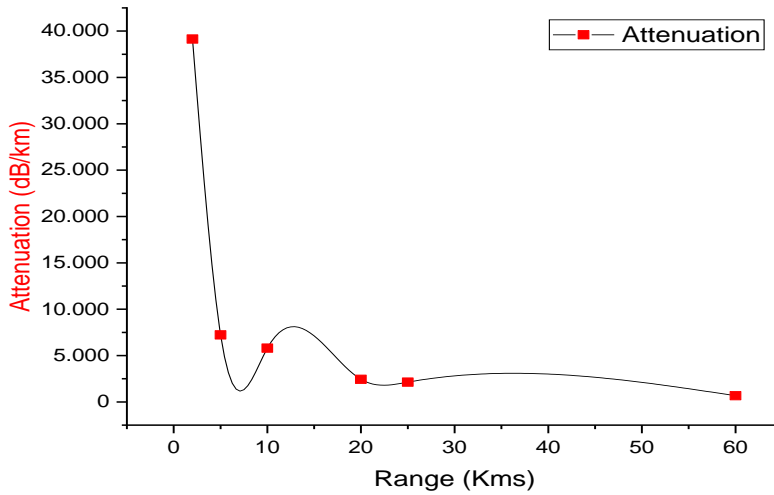


Figure 4.3: Attenuation versus visibility range plot for rain

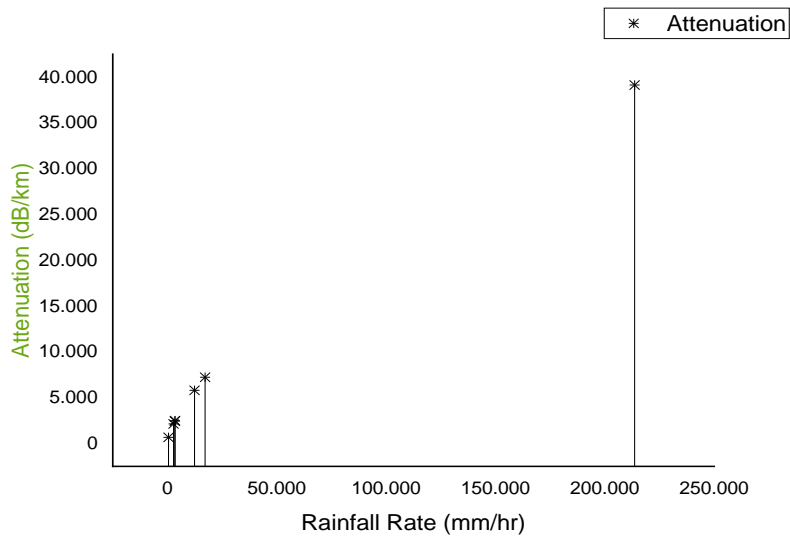


Figure 4.4: Rainfall rate versus attenuation plot for rain

In this chapter, two weather conditions have been analysed which are dust and rain. The change of attenuation versus the visibility range is shown through different plots for each

weather. The rainfall rate has been observed for Jaipur city from year 2015 (highest) to 2021 with its changing range each year. The observations are shown in Table 4.1 and 4.2. The same data has been kept in Opti system software while doing the simulations.

4.1: WDM OWC SYSTEM SIMULATIONS

This chapter discusses the simulation work carried out to design optical wireless communication (using OWC channel) system using hybrid configuration of EDFA amplifiers to make it more efficient than FSO (FSO channel) in dense climatic conditions.

The system was designed using Opti system 7.0 software. The reason for using 1550nm wavelength is because of its low attenuation properties. The beam divergence of the system is set to 2.5 mrad, and the aperture size at receiver end is set to 30 cm. The system is built with amplifiers in the WDM network in mind. The amplifier has a gain of 50 dB. This paper has discussed three configurations of the system.

In system config.-I, three optical amplifiers were used. It's a three-channel WDM OWC system with the ability to expand the number of channels based on user demand. As shown in Figure 4.1.1, it employs an optical amplifier on the transmitter side in a post-amplifier configuration. Before the WDM, the message is amplified, and then it is forwarded for multiplexing. The channel is joined and the output is depicted using a corresponding multiplexer and de-multiplexer.

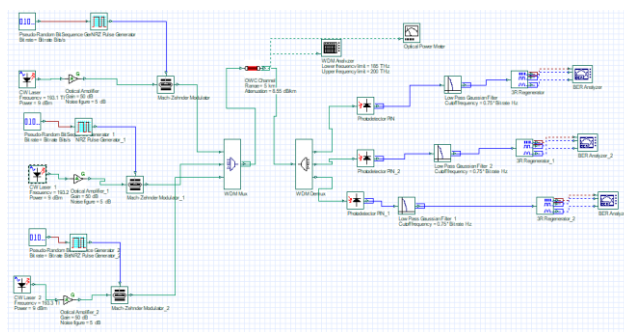


Figure 4.1.1: System config. I simulation using three optical amplifiers

Two optical amplifiers are used in system config.-II. The setup is similar to the previous config. of the system, but the amplifier is in a distant region. Analysers are then used to examine the output. Figure 4.1.2 depicts system config.-II's design layout. The amplifiers are used in two different ways. It is unaffected by the number of consumers because, irrespective of how many are implemented, only two channels are used.

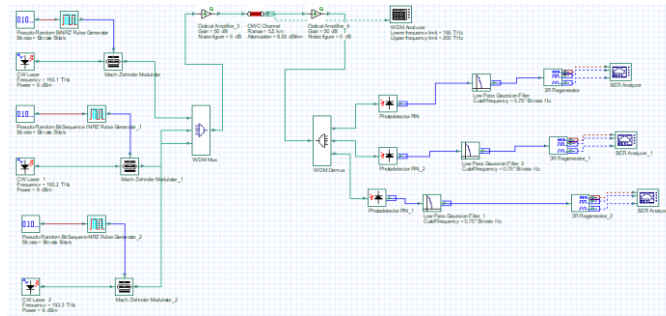


Figure 4.1.2: System config. II simulation using two optical amplifiers

Although, there is no significant difference in the performance of the system with 2 or 3 optical amplifiers. However, a better system configuration is presented that employs a hybrid amplifier configuration. Figure 4.1.3 depicts the situation. As can be seen, that the proposed system combines both system config.-I and system config -II. The hybrid system configuration was chosen because it yields a high gain from the combination and has a higher channel handling capacity. The advantages of both configurations can be obtained by combining them.

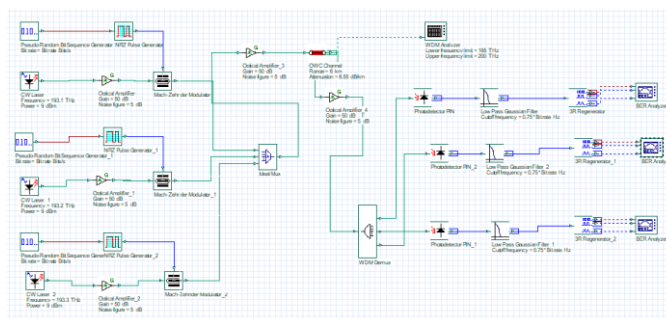


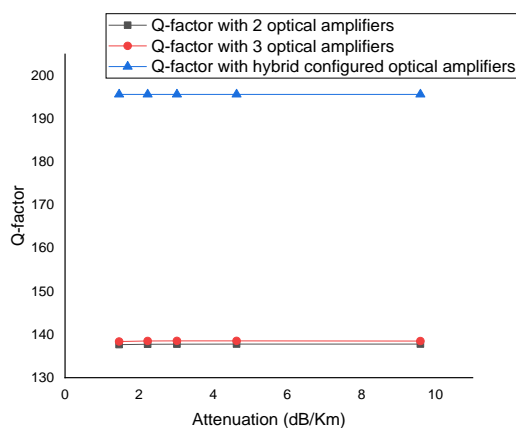
Figure 4.1.3: Simulation of hybrid configuration of the system

Different configurations using optical amplifiers (EDFA) are discussed and simulated in this chapter. Among all the configurations i.e., pre, post and hybrid, the hybrid configuration of EDFAs is more robust to provide high Q-factor and less BER.

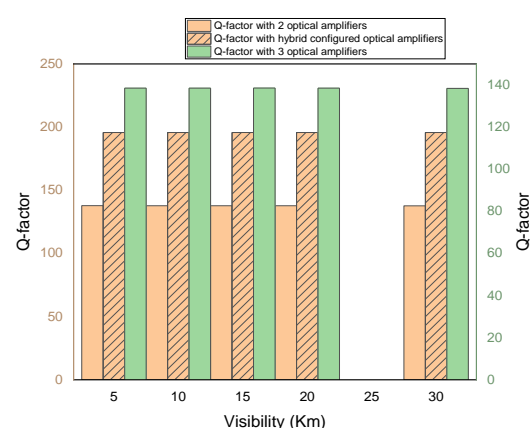
4.2: RESULTS FOR WDM OWC SYSTEM UNDER DIFFERENT WEATHER CONDITIONS

The outcomes of simulated models of section 4.1 are shown in this section. Moreover, this chapter also discusses how the Q-factor is changing with respect to attenuation and visibility range for each weather condition. The performance of all the EDFA configurations using OWC channel is compared by using different plots.

Two system configurations are compared in this study, under dusty and rainy climatic conditions. System config.-I have a post-amplifier configuration, and the number of op-amps used in this configuration are determined by the number of users required. Three users are considered in this analysis. Only two amplifiers are used in System config.-II, one following WDM at the transmitter and the other preceding WDM at the receiver. According to the different weather conditions applied, it is observed that system config.-II is providing better quality factor over system config.-I. Both the system configurations are combined for hybrid system configuration and the hybrid optical amplifier configuration is found to have the highest Q-factor.



(a)



(b)

Figure 4.2.1: Q-factor plot of Dust at 2.5 Gbps (a) against attenuation (b) against visibility range.

The Figure 4.2.1 is showing Q-factor changes for dusty weather condition at 2.5 Gbps of bit rate. The signal quality is changing with respect to the attenuation and range of visibility. The Q-factor of system config.-II is comparable to config.-I and Q-factor of hybrid system config. is highest. The obtained bit error rate (BER) is 0 for all the three system configurations. Figure 4.2.2 is showing eye diagrams for system config.-I, II and hybrid configured optical amplifiers under storm/dust.

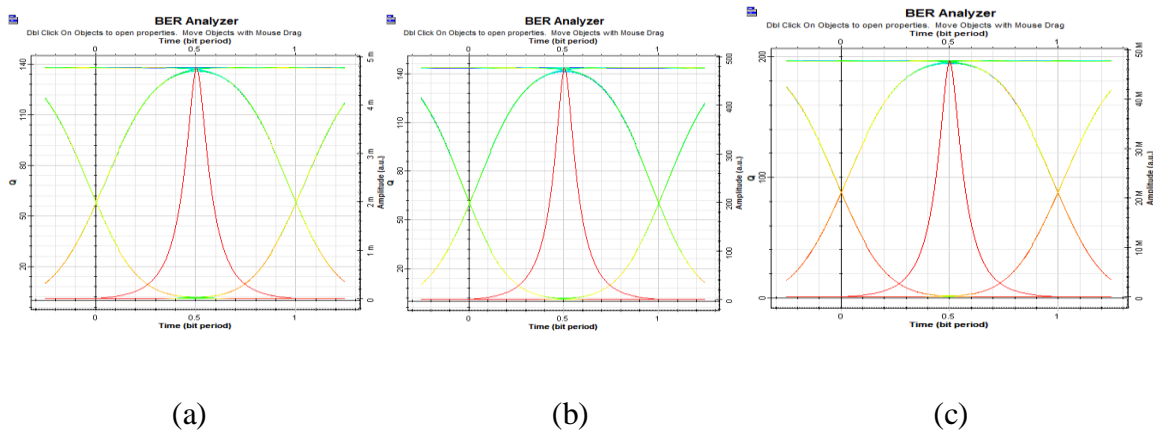


Figure 4.2.2: Eye-diagram plot of dusty weather for: (a) System config.-I (b) System config.-II (c) Hybrid System config.

The changes in attenuation for rain are noted according to different years of rainfall rate and based on the equation. Different visibility range provided different values for attenuation and average attenuation is calculated for all years. The obtained attenuation is 8.55 dB/km.

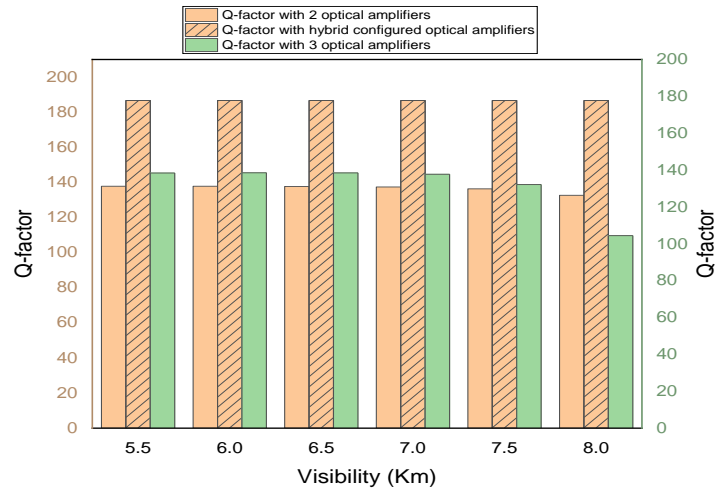


Figure 4.2.3: Q-factor versus visibility range plot for Rain at 2.5 Gbps

The Figure 4.2.3 is showing the average Q-factor for rain at 1550 nm and 2.5 Gbps. The obtained BER is 0. The Q-factor is decreasing as the range is increasing and it is slightly better for system config.-I as compared to system config.-II and the maximum value is obtained for hybrid config. throughout the range. Figure 4.2.4 is showing the eye diagram for different systems under rainy weather condition.

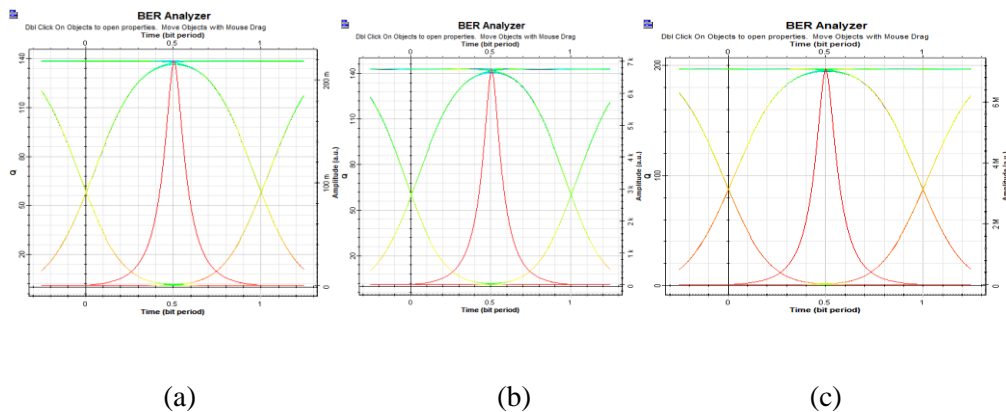


Figure 4.2.4: Eye-diagram plot of rainy weather for: (a) System config.-I (b) System config.-II (c) Hybrid System config.

The results show that the hybrid configuration of EDFA using OWC channel is improving the Q-factor and BER much more and is proved to be working better in dense climatic

conditions. The eye-statures of all the configurations are shown and the larger eye-opening is observed in hybrid configuration which shows that the retrieved signal has high quality and minimum errors.

CHAPTER-5

SYSTEM ARCHITECTURE OF ASK AND PSK MODULATION TECHNIQUES

This chapter deals with the research work for enhancement of coupler-based delay line filters modulation techniques using optical wireless channel and amplifiers at 100 Gbit/s. The block diagrams are shown for the proposed systems for each modulation technique by using new components like OWC channel and EDFA amplifiers. The optical amplifiers used are in hybrid configuration with gain of 50 dB so that they can increase the signal amplification.

5.1.ASK MODULATION TECHNIQUE WITH HOAS

Figure 5.1.1 presents a block diagram of the proposed OWC system, that implements ASK modulation as well as a hybrid configuration of optical EDFA amplifiers.

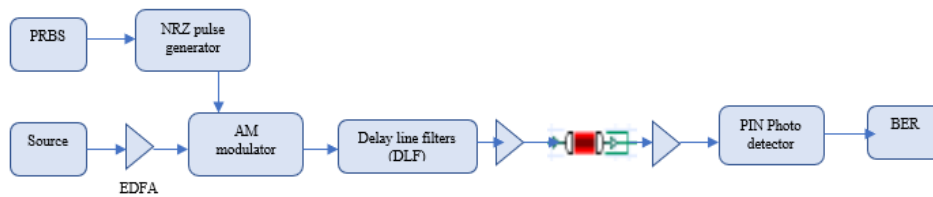


Figure 5.1.1: ASK modulated OWC system using HOAs.

The first stage is the transmitter, which includes a continuous wave laser, an optical amplifier with a gain of 50 dB, an AM modulator, a pseudo-random bit sequence generator, and an NRZ pulse generator. The NRZ pulse generator encodes the digital data from the bit sequence generator and modulates the amplified signal from the laser via the AM modulator. The following stage includes delay line filters, which are used to compensate for the dispersion effects caused by atmospheric turbulence [35]. The coupler's coupling coefficients are used to change the dispersion slope, and the dispersion slope value can be designed accordingly [36]. To improve signal quality, the central stage is an OWC channel connected

to two optical amplifiers. Last stage consists receiver where the optical detector detects the signal and converts it to the electrical signal. The receiver is the final stage, where the optical detector detects the signal and converts it to an electrical signal.

5.2.PSK MODULATION TECHNIQUE WITH HOAS

Figure 5.2.2 presents a diagram of the proposed OWC system, that implements PSK modulation as well as a hybrid configuration of optical EDFA amplifiers.

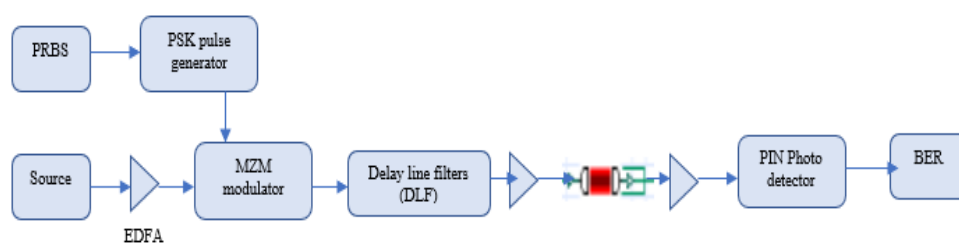


Figure 5.2.2: PSK modulated OWC system using HOAs.

The first stage is the transmitter, which includes a continuous wave laser, an optical amplifier with a gain of 50 dB, a Mach Zehnder modulator (MZM), a pseudo-random bit sequence generator, and a PSK pulse generator. The PSK pulse generator encodes the digital data from the bit sequence generator and modulates the amplified signal from the laser via the MZM modulator. The following stage includes delay line filters, which are used to compensate for the dispersion effects caused by atmospheric turbulence. The coupler's coupling coefficients are used to change the dispersion slope, and the dispersion slope value can be designed accordingly [36]. To improve signal quality, the central stage is an OWC channel connected to two EDFA amplifiers. Last stage consists receiver where the optical detector detects the signal and converts it to the electrical signal. The receiver is the final stage, where the optical detector detects the signal and converts it to an electrical signal.

Section 5.1 and 5.2 discussed the block diagram of proposed system. The components used at the transmitter, channel and how they are working is discussed.

5.3: OWC DESIGN SIMULATIONS

In this chapter simulations are shown for the proposed design of ASK and PSK coupler-based delay line filters modulation techniques. OWC channel is used in place of FSO channel to make system more robust under climatic conditions and EDFA optical amplifiers are added in the hybrid configuration to enhance the system performance

5.3.1. ASK MODULATED OWC DESIGN SIMULATION

Figure 5.3.1 depicts the simulation of an ASK modulation OWC system using HOAs under various climatic conditions using Opti system software. The optical transmitter is made up of a Pseudo-Random Binary Sequence (PRBS) generator that generates data bits at a bit rate of 10Gbits/sec. This is encoded with a Non-Return to Zero (NRZ) pulse generator. A continuous-wave laser with a power of 9 dBm and a frequency of 193.1 THz is amplified and modulated by encoded bits via an EDFA amplifier and an optical amplitude modulator. The modulator's output is the optical signal, which is fed into the delay line filter via x-couplers. Depending on the coupling coefficient, the first coupler divides the input signal into two. One of the split signals is phase-shifted, while the other is not. Then, at the second coupler, they are recombined. These are split, time-delayed, and phase-shifted yet again. Finally, they are combined at the third coupler to receive the compensated signal. The free space medium (OWC channel) connected to EDFA amplifiers is analysed under various climate conditions by varying the range. A PIN photodiode and a 3R-regenerator are used in the optical receiver. The PIN photodiode converts the received optical signal into an electrical signal [37]. The original bit sequence is stored in the 3R-regenerator. The results are analysed using oscilloscope visualizers and bit error rate (BER) analysers.

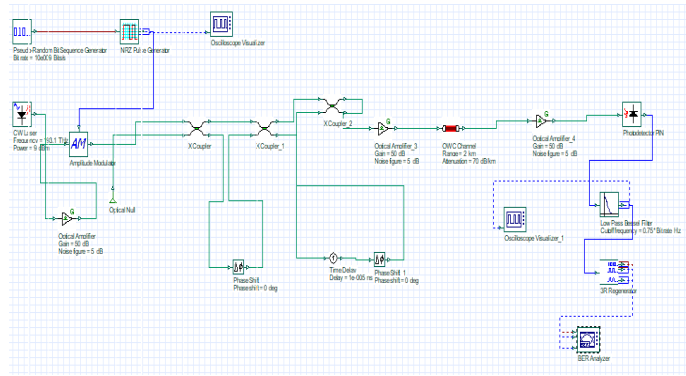


Figure 5.3.1. Simulation of HOAs based ASK modulated OWC system

5.3.2. PSK MODULATED OWC DESIGN SIMULATION

Figure 5.3.2 depicts the simulation of a PSK modulation OWC system using HOAs under various climatic conditions using Opti system software. The optical transmitter generates data bits at a rate of 10 Gbits/sec using a PRBS generator, which is then encoded using a PSK pulse generator. To generate the optical carrier signal, a CW laser with a power of 9 dBm and a frequency of 193.1 THz was used. The output of the PSK pulse generator modulates the EDFA amplified optical carrier signal with an MZM modulator to produce the PSK modulated signal. As previously explained, the modulated signal is passed through the delay line filter to improve the performance of the OWC system. The compensated signal is routed through the OWC channel, which is linked to amplifiers. The performance is evaluated by using various ranges and attenuation values of the OWC channel that correspond to various climatic conditions. To obtain the original bit sequence in electrical signal form, the optical receiver has a PIN photodiode and a 3R-regenerator. Finally, the performance is evaluated using oscilloscope visualizers and a BER analysers.

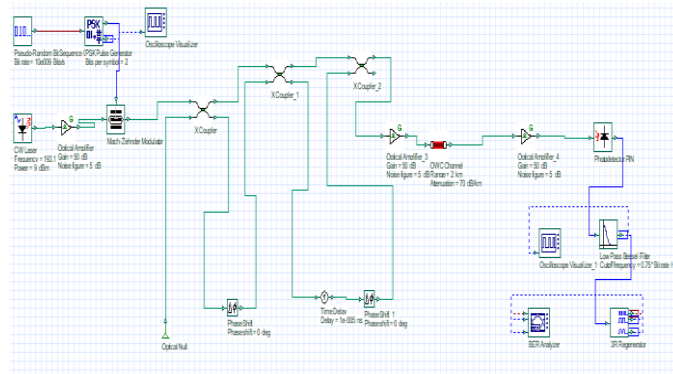


Figure 5.3.2. Simulation of HOAs based PSK modulated OWC system.

This chapter has discussed the Opti system simulation for OWC system using HOAs and modulation techniques. Section 5.3.1 discussed the proposed amplitude shift keying modulation based on DLF. The data rate of the system is changed from 10 Gbit/s to 100 Gbit/s to check the simulation results. Similarly, section 5.3.2 discussed the proposed phase shift keying modulation based on DLF with same data rate of 10Gbit/s to 100 Gbit/s. The comparative simulation results for both the systems are further discussed in section 5.4.

5.4: RESULTS FOR DLF BASED MODULATION TECHNIQUES USING OWC CHANNEL AND AMPLIFIERS

In this chapter, different results are shown in tabular form for different climatic conditions. The results are based on the simulations done in section 5.4. Moreover, the comparison is also made for the reference system and the proposed system under similar climatic conditions.

In [38]-[39], the author described the effects of various weather conditions for different atmospheric turbulences such as rain, fog, haze, and so on, as well as the maximum visibility range and attenuation present for such climatic conditions. Table 5.4.1 shows the parameters of the FSO system under various conditions. Tables 5.4.2-5.4.5 show the OWC channel using HOAs system parameters for various climatic conditions such as haze, rain-mist, snow, and medium fog.

Table 5.4.1 Atmospheric parameters under different climate for free space optics communication

Atmospheric Condition	Attenuation (dB/km)
Haze	20
Rain and mist	30
Snow	40
Medium Fog	70

Table 5.4.2. Output for Haze condition

Work	Attenuation (dB/Km)	Range (m)	Q-factor	BER	Bit rate (Gbps)
ASK (ref.)	20	3500	56.5069	0	10
PSK (ref.)	20	3500	57.0486	0	10
ASK (Proposed)	20	5000	113.373	0	100
PSK (Proposed)	20	5000	357.637	0	100

Table 5.4.3. Output for rain and mist condition

Work	Attenuation (dB/Km)	Range (m)	Q-factor	BER	Bit rate (Gbps)
ASK (ref.)	30	2500	31.4472	2.29e-217	10
PSK (ref.)	30	2500	34.039	2.85e-254	10
ASK (Proposed)	30	4000	62.457	0	100
PSK (Proposed)	30	4000	86.83	0	100

Table 5.4.4. Output for snow condition

Work	Attenuation (dB/Km)	Range (m)	Q-factor	BER	Bit rate (Gbps)
ASK (ref.)	40	1900	44.994	0	10
PSK (ref.)	40	1900	46.139	0	10
ASK (Proposed)	40	3000	75.524	0	100
PSK (Proposed)	40	3000	115.009	0	100

Table 5.4.5. Output for medium fog condition

Work	Attenuation (dB/Km)	Range (m)	Q-factor	BER	Bit rate (Gbps)
ASK (ref.)	70	1200	16.114	1.004e-058	10
PSK (ref.)	70	1200	17.535	3.84e-069	10
ASK (Proposed)	70	2000	18.708	1.52e-078	20
PSK (Proposed)	70	2000	22.1501	5.065e-109	50

For haze conditions, the proposed HOAs-based ASK modulation and PSK modulation have 5000 m line of sight and a high-quality factor of 113.373 and 357.637 at higher bit rates of 100 Gbps, respectively.

For rain and mist conditions, the proposed HOAs-based ASK modulation and PSK modulation have 4000 m line of sight and a high-quality factor of 62.457 and 86.83 at bit rate of 100 Gbps, respectively.

For snow conditions, the proposed HOAs-based ASK modulation and PSK modulation have a 3000 m line of sight and a high-quality factor of 75.524 and 115.009 at 100 Gbps bit rate, respectively.

For medium fog conditions, the proposed HOAs-based ASK modulation and PSK modulation have a 2000 m line of sight and a high-quality factor of 18.708 at 40 Gbps and 22.1501 at 50 Gbps of bit rate, respectively.

Eye diagrams for various climatic conditions of HOAs based ASK modulation with DLF and PSK modulation with DLF are mentioned in Figure 5.4.1 and Figure 5.4.2 that include maximum quality factor, minimum BER and threshold.

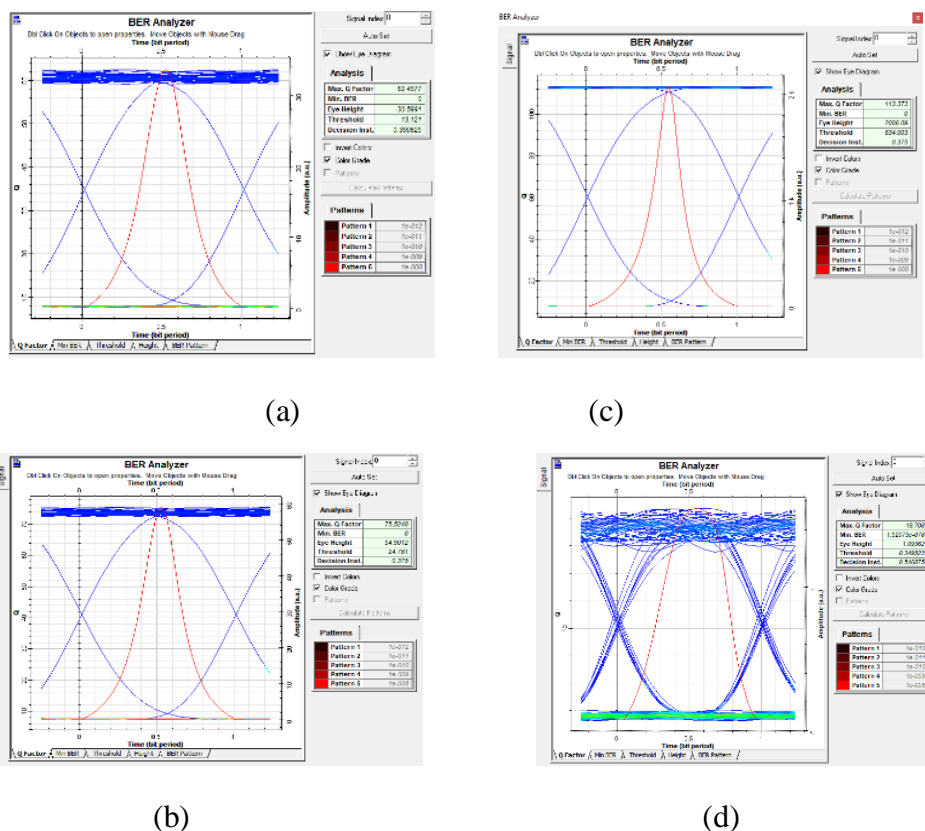


Figure 5.4.1. Eye-diagrams for HOAs based ASK OWC system under (a) Haze, (b) Snow, (c) Rain and mist, (d) Medium fog condition.

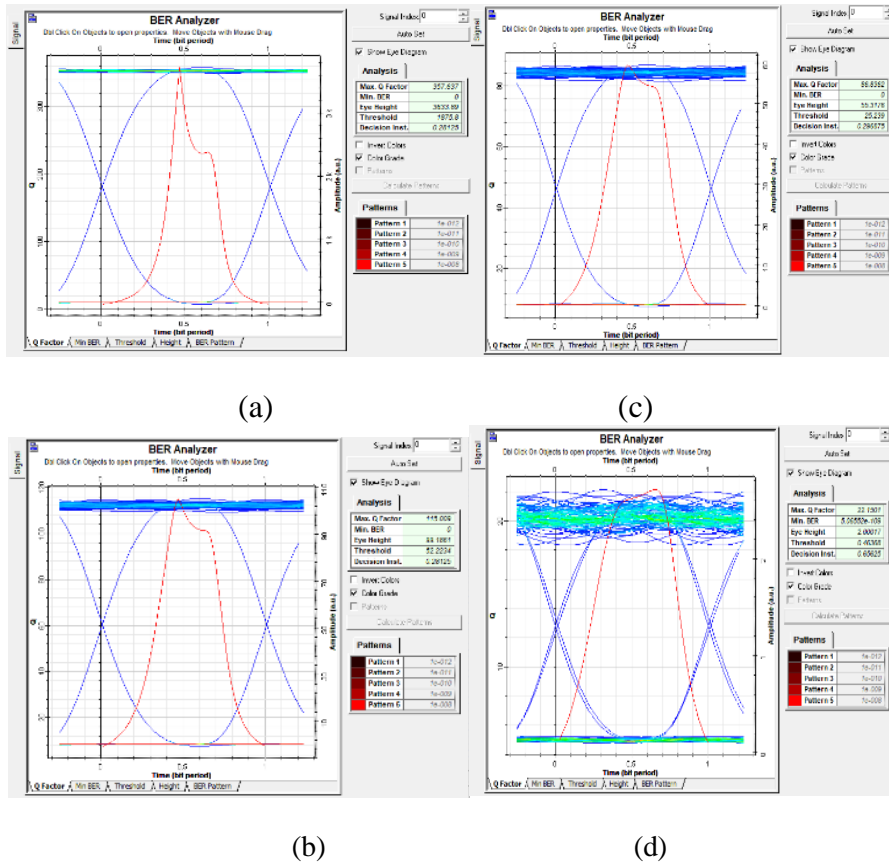


Figure 5.4.2. Eye-diagrams for HOAs based PSK OWC system under (a) Haze, (b) Snow, (c) Rain and mist, (d) Medium fog condition.

The results shown in tabular form are proving that the proposed system is working much better with the reference system where FSO channel was used without optical amplifiers. The proposed system using OWC channel can be used in dense weather conditions also at higher data rates with good Q-factor and BER almost to zero. The eye-statures shown in Figure 5.4.1 and Figure 5.4.2 are proving the error free signal of good quality factor with larger eye opening.

CHAPTER-6

CONCLUSION AND SCOPE

This chapter provides the conclusion for the research work done to reduce dispersion (Chapter2 -6), to make wireless optical communication using OWC channel (Chapter7-9), and to design ASK and PSK coupler-based delay line filters modulation techniques using OWC channel and amplifiers at 100 Gbit/s (Chapter 10-12).

6.1.CONCLUSION OF RESEARCH FOR DISPERSION COMPENSATION

The work carried out in this research is mainly focused on reducing the chromatic dispersion in the signal by using the DCF and cascaded FBG concepts with a system bit rate of 10 Gbps for 120 kilometres of SMF fibre. Overall observation shows that introduction of cascaded FBG technique with DCF technique is useful in reducing the dispersion of the system and to obtain better quality of the signal. Among different DCF techniques, the post-DCF is providing the highest Q-factor of 35.987 at 10 Gbps and pre-DCF is providing minimum BER of -71.707 at 10 Gbps. The maximum percentage change in Q-factor and BER is 35.38% and 86.85% obtained for post-DCF technique. The comparative plots and figures are presented for amplitude modulated signal as well. Among different DCF techniques, the post-DCF is providing the highest Q-factor of 36.961 minimum BER of -975.187 dB at 10 Gbps. The maximum percentage change in Q-factor and BER is 38% and $\approx 100\%$ respectively obtained for post-DCF technique. It is concluded that using cascaded FBGs with post-DCF technique can lower down the dispersion better for 120 km length of fibre and is also providing good Q-factor.

6.2.CONCLUSION OF RESEARCH FOR WDM OWC CHANNEL WITH EDFA HYBRID CONFIGURATION

Due to the numerous benefits, it provides, OWC is advancing in a variety of fields. The system, which is made up of a hybrid combination of amplifiers is accessible at data rate of 10 Gbps. The attenuation and range of the OWC channel are changed accordingly to the dusty and rainy weather conditions. The Q-factor obtained is approximately same with two optical amplifier and three optical amplifier configuration and it is obtained 198 (highest) for hybrid configuration of the system. Moreover, the hybrid configuration of WDM OWC system is simulated at 10Gbit/s with signal wavelength of 1550 nm and it provides average values of Q-factor and BER; 10.878 and -114.667 dB (10^{-027}) respectively, which satisfies the basic limit of Q-factor (>6) and BER ($<10^{-009}$). Under different climatic conditions, the presented WDM OWC system based on hybrid optical amplifier configuration has shown to be a premium and effective system. This system can be used in states like Rajasthan where the atmospheric conditions are extreme and dust storms are more frequent.

6.3.CONCLUSION OF RESEARCH ON “ENHANCEMENT OF COUPLER-BASED DELAY LINE FILTERS MODULATION TECHNIQUES USING OPTICAL WIRELESS CHANNEL AND AMPLIFIERS AT 100 GBIT/S”

An improvement in the performance of an ASK and PSK modulation techniques with coupler-based delay line filter is presented by utilising hybrid configuration of optical amplifiers and OWC channel under various climatic conditions which is providing high Q-factor and BER to almost zero. The proposed study is compared to previous studies conducted under similar conditions. At bit rates up to 100 Gbps, the HOAs-based PSK modulated OWC system is found to be more efficient than the ASK modulated OWC system.

The overall research work done here can be used to implement those systems which can improve the Q-factor and BER by reducing dispersion using FBGs and DCF fibres, by enhancing the channel capacity using OWC channel and by increasing the message signal

intensity using EDFA amplifiers under different climatic conditions like rain, dust, haze, snow, fog.

REFERENCES

- [1]Ashwani Sharma, Inder Singh, Suman Bhattacharya and Shalini Sharma 2019 Performance Comparison of DCF and FBG as Dispersion Compensation Techniques at 100 Gbps Over 120 km using SMF *Springer Nature Singapore Pte Ltd. Lecture Notes in Electrical Engineering 511*. https://doi.org/10.1007/978-981-13-0776-8_40.
- [2]Ahmed F. Sayed, Fathy M. Mustafa, Ashraf A. M. Khalaf1 · Moustafa H. Aly 2020 An enhanced WDM optical communication system using a cascaded fiber Bragg grating *Optical and Quantum Electronics 52:181* <https://doi.org/10.1007/s11082-020-02305-9>.
- [3]J.Karunya, Dr.P.Prakash 2017 Analysis of WDM system using DCF *4th International Conference on Signal Processing, Communications and Networking (ICSCN -2017), March 16 – 18, Chennai, INDIA*.
- [4]Fauza Khair, I Wayan Mustika, Fahmi, Dodi Zulherman, Fakhriy Hario 2018 Comparative Analysis of Dispersion Compensating Fiber in DWDM System using 10 Gbps and 40 Gbps Bit Rate *10th International Conference on Information Technology and Electrical Engineering (ICITEE)*.
- [5] Natalia M. Litchinitser, Benjamin J. Eggleton, and Govind P. Agrawal, Fellow, IEEE, Fellow, OSA, 1998 Dispersion of Cascaded Fiber Gratings in WDM Lightwave Systems *JOURNAL OF LIGHTWAVE TECHNOLOGY, VOL. 16, NO. 8*.
- [6]Bedir Yousif, Ahmed Sh. Samrahb, and Rawan Waheed 2020 High Quality Factor and Dispersion Compensation Based on Fiber Bragg Grating in Dense Wavelength Division Multiplexing *ISSN 1060-992X, Optical Memory and Neural Networks, Vol. 29, No. 3, pp. 228–243. © Allerton Press, Inc.*
- [7]**Nath**, Vijay, **Mandal** and J.K 2019 Nanoelectronics, communications and circuits system *Springer science and business media ltd, proceeding of NCCS*.

- [8] CHEN, Shiyu LI, Peixiang LU, Dongxiang WANG and Wenyong LUO
2010 Dispersion compensation optical fiber modules for 40 Gbps WDM communication systems *Front Optoelec Chin*, 2010, 3(4): 333–338 <https://doi.org/10.1007/s12200-010-0117-6>.
- [9] <https://optiwave.com/optisystem-overview/>
- [10] Fauza Khair , Wayan Mustika, Fahmi, Dodi Zulherman, Fakhriy Hario, “Comparative Analysis of Dispersion Compensating Fiber in DWDM System Using 10 Gbps and 40 Gbps Bit Rate”, 2018 10th International Conference on Information Technology and Electrical Engineering (ICITEE).
- [11] Govind P. Agrawal,” FIBER-OPTIC COMMUNICATION SYSTEMS”, The Institute of Optics University of Rochester Rochester, New York.
- [12] B. J. Eggleton, G. Lenz, N. Litchinitser, D. B. Patterson, and R. E. Slusher, “Implications of Fiber Grating Dispersion for WDM Communication Systems”, IEEE PHOTONICS TECHNOLOGY LETTERS, VOL. 9, NO. 10, OCTOBER 1997.
- [13] Craig Warren and Antonios Giannopoulos, “Experimental and Modeled Performance of a Ground Penetrating Radar Antenna in Lossy Dielectrics,” IEEE JOURNAL OF SELECTED TOPICS IN APPLIED EARTH OBSERVATIONS AND REMOTE SENSING, VOL. 9, NO. 1, JANUARY 2016.
- [14] Lihan Wang, Yijie Fang, Shupeng Li, Xiangchuan Wang, and Shilong Pan, Senior Member, IEEE, “FBG Demodulation with Enhanced Performance based on Optical Fiber Relative Delay Measurement,” DOI 10.1109/LPT.2020.2995363, IEEE Photonics Technology Letters 2020.
- [15] Farhana Hossain, Zeenat Afroze, “Eliminating the effect of Fog attenuation on FSO link by multiple TX/RX system with travelling wave semiconductor optical amplifier” in

- International Conference on Advances in Electrical Engineering (ICAEE 2013), pp. 267-272, dec. 2013.
- [16] Ghassemlooy, Z. and Popoola, W.O., "Terrestrial Free-Space Optical Communications," in *Mobile and Wireless Communications: Network layer and circuit level design*, pp. 355-391
- [17] Wan Rizul Hazman Wan Ruslan, Sevia Mahdaliza Idrus, Arnidza Ramli, Norhafizah Ramli, Abu Sahmah Mohd Supa'at, Farizal Mohd Nor, "Terrestrial Free Space Optic Propagation Analysis Considering Malaysia Weather Condition," in *Journal Technology*, pp. 217-229, January 2011.
- [18] Navneet Dayal, Preeti Singh¹, Pardeep Kaur, "Long Range Cost-Effective WDM-FSO System Using Hybrid Optical Amplifiers" Springer Science and Business Media, LLC 2017, Wireless Pers Commun DOI 10.1007/s11277-017-4826-7.
- [19] Maged Abdullah Esmail, Habib Fathallah, and Mohamed-Slim Alouini, "Effect of Dust Storms on FSO Communications Links," *Computer, Electrical, and Mathematical Science and Engineering (CEMSE) Division, King Abdullah University of Science and Technology (KAUST) Thuwal, Makkah Province, Saudi Arabia.*
- [20] Artolink, 10 Gbit/s Artolink model. Available: http://artolink.com/page/products/free_space_optics_Artolink_10Gbps/.
- [21] M. A. Esmail, H. Fathallah, and M. S. Alouini, "Outdoor FSO Communications under Fog: Attenuation Modeling and Performance Evaluation," *IEEE Photonics Journal*, vol. 8, pp. 1-22, 2016.
- [22] Dayal, N., Singh, P., & Kaur, P. (2015), "Performance enhancement in WDM-FSO system using optical amplifiers under different rain conditions", In *ICICCD*. Springer.

- [23] Jain, P., Vashist, K., & Gupta, N. (2014), “Comparison study of hybrid optical amplifier. International Journal of Scientific Research Engineering and Technology”, 3(9), 1289–1292.
- [24] Kshatriya, A. J., Acharya, Y. B., & Aggarwal, A. (2013), “Analysis of free space optical link in Ahmedabad weather conditions” In Proceedings of 2013 IEEE Conference on Information and Communication Technologies.
- [25] Nadeem, F., Leitgeb, E., Awan, M. S., & Chessa, S. (2009), “Comparing lifetime of terrestrial wireless sensor network by hybrid FSO/RF and only RF”, In 2009 Fifth International Conference on Wireless and Mobile Communication. IEEE.
- [26] Nadeem, F., & Leitgeb, G. (2010), “Dense maritime fog attenuation prediction from measured visibility data”, Radio Engineering, 19(2), 223–227.
- [27] International Electrotechnical Commission Standard: Safety of optical fibre communication systems (IEC, 2018). <https://webstore.iec.ch/publication/62241>.
- [28] Bobrovs, V., Olonkins, S., Ozolins, O., Porins, J., & Lauks, G. (2012), “Hybrid optical amplifiers for flexible development in long reach optical access system”, In 3rd Fiber Optics in Access Network— FOAN (pp. 577–582).
- [29] Fadhil, H. A., Amphawan, A., Shamsuddin, H. A. B., Abd, T. H., Al-Khafaji, H. M. R., Aljunid, S. A., et al. (2013). Optimization of free space optics parameters: An optimum solution for bad weather conditions. Optik-International Journal for Light and Electron Optics, 124(19), 3969–3973.
- [30] Jain, P., Vashist, K., & Gupta, N. (2014), “Comparison study of hybrid optical amplifier”, International Journal of Scientific Research Engineering and Technology, 3(9), 1289–1292.
- [31] <https://optiwave.com/optisystem-overview/>

- [32] Farhana Hossain, Zeenat Afroze, “Eliminating the effect of Fog attenuation on FSO link by multiple TX/RX system with travelling wave semiconductor optical amplifier” in International Conference on Advances in Electrical Engineering (ICAEE 2013), pp. 267-272, dec. 2013.
- [33] Navneet Dayal, Preeti Singh¹, Pardeep Kaur, “Long range cost-effective WDM-FSO system using hybrid optical amplifiers” Springer Science and Business Media, LLC 2017, Wireless Pers Commun DOI 10.1007/s11277-017-4826-7.
- [34] *International Electrotechnical Commission Standard: Safety of optical fibre communication systems* (IEC, 2018). <https://webstore.iec.ch/publication/62241>.
- [35] Mohd Ashraf, Gaurav Baranwal, Dinesh Prasad, Saima Idris, Mirza Tariq Beg, “Performance analysis of ASK and PSK modulation based FSO system using coupler-based delay line filter under various weather conditions”, Optics and Photonics Journal, 2018, 8, 277-287 <http://www.scirp.org/journal/opj>, ISSN Online: 2160-889X.
- [36] Duthel, T., et al. (2006), “Quasi-analytic synthesis of non-recursive optical delay line filters for reliable compensation of dispersion effects”, Journal of Lightwave Technology, 24, 4403-4410. <https://doi.org/10.1109/JLT.2006.88147>.
- [37] Ashraf, M. and Ranjan, R. (2018), “Tunable single passband microwave photonic filter based on direct generation technique”, 3rd International Conference on Microwave and Photonics (ICMAP), Dhanbad, 9-11 February 2018, 1-2. <https://doi.org/10.1109/ICMAP.2018.8354521>.
- [38] Vavoulas, A., Sandalidis, H.G. and Varoutas, D. (2012), “Weather effects on FSO network connectivity”, IEEE/OSA Journal of Optical Communications and Networking, 4, 734-740. <https://doi.org/10.1364/JOCN.4.000734>

- [39] Nebuloni, R. and Capsoni, C. (2016), “Effects of adverse weather on free space optics”, In: Uysal, M., et al., Eds., *Optical Wireless Communications, Signals and Communication Technology*, Springer International Publishing, Switzerland, 47-68.

LIST OF PUBLICATIONS

1. Divya Sisodiya, Deepika Sipal, “Long range and low cost WDM OWC system with hybrid configuration of optical amplifiers”, IEEE ICAECT 2022, Bhillai, Chhattisgarh (accepted and presented).
2. Divya Sisodiya, Deepika Sipal, “modelling and performance analysis of cascaded FBGs with different DCF techniques at 10 Gbps”, journal of optical communications. (Under second revision)
3. Divya Sisodiya, Deepika Sipal, “Enhancement of ASK and PSK modulation based on coupler-based delay line filters using OWC channel and EDFA amplifiers at 100 Gbit/s”, ICCIT 2022 New York, United States <https://waset.org/communication-and-information-technology-conference-in-june-2022-in-new-york>. (accepted)